

The European Journal of Neuroscience

Volume 3 Number 7 July 1991

CONTENTS

RESEARCH PAPERS

- Mediodorsal Thalamic Lesions Impair Long-Term Visual Associative Memory in Macaques
D. Gaffan and S. Watkins 615
- NMDA Actions on Rat Abducens Motoneurons
J. Durand 621
- Molecular Association of the Neural Adhesion Molecules L1 and N-CAM in the Surface Membrane of Neuroblastoma Cells is Shown by Chemical Cross-linking
H. Simon, S. Klinz, T. Fahrig and M. Schachner 634
- Innervation of Entorhinal Principal Cells by Neurons of the Nucleus Reuniens Thalami. Anterograde PHA-L Tracing Combined with Retrograde Fluorescent Tracing and Intracellular Injection with Lucifer Yellow in the Rat
F. G. Wouterlood 641
- Auditory Pontine Grey: Connections and Response Properties in the Horseshoe Bat
G. Schuller, E. Covey and J. H. Casseday 648
- Modulation of Human Neurite Outgrowth by Serine Proteases: A Comparison of the Interaction of Thrombin and Prothrombin with Glia-Derived Nexin
P. W. Grabham, D. Monard, P. H. Gallimore and R. J. A. Grand 663
- Characterization and Regional Distribution of a Class of Synapses with Highly Concentrated cAMP Binding Sites in the Rat Brain
A. Caretta, D. Cevolani, G. Luppino, M. Matelli and R. Tirindelli 669
- Cells that Express Brain-Derived Neurotrophic Factor mRNA in the Developing Postnatal Rat Brain
W. J. Friedman, L. Olson and H. Persson 688
- Nerve Growth Factor is Required for Induction of c-Fos Immunoreactivity by Serum, Depolarization, Cyclic AMP or Trauma in Cultured Rat Sympathetic Neurons
A. Buckmaster, C. D. Nobes, S. N. Edwards and A. M. Tolkovsky 698
- SHORT COMMUNICATION
- Calcitonin Gene-related Peptide Stimulates the Induction of c-fos Gene Expression in Rat Astrocyte Cultures
C. A. Haas, M. Reddington and G. W. Kreutzberg 708
- ERRATUM 713

The European Journal of Neuroscience

Volume 3 Number 8 August 1, 1991

CONTENTS

RESEARCH PAPERS

- AMPA Neurotoxicity in Rat Cerebellar and Hippocampal Slices: Histological Evidence for Three Mechanisms
G. Garthwaite and J. Garthwaite 715
- Mechanisms of AMPA Neurotoxicity in Rat Brain Slices
G. Garthwaite and J. Garthwaite 729
- Calcitonin Gene-related Peptide (CGRP)-like Immunoreactivity and CGRP mRNA in Rat Spinal Cord Motoneurons after Different Types of Lesions
F. Piehl, U. Arvidsson, H. Johnson, S. Cullheim, M. Villar, Å. Dagerlind, L. Terenius, T. Hökfelt and B. Ulfhake 737
- Expression of Human Neurofilament-light Transgene in Mouse Neurons Transplanted into the Brain of Adult Rats
M. Vidal-Sanz, M. P. Villegas-Pérez, D. A. Carter, J.-P. Julien, A. Peterson and A. J. Aguayo 758
- Immunohistochemistry of *c-fos* in Mouse Brain During Postnatal Development: Basal Levels and Changing Response to Metrazol and Kainate Injection
Y. Sakurai-Yamashita, P. Sassone-Corsi and G. Gombos 764
- Properties of a High-threshold Voltage-activated Calcium Current in Rat Cerebellar Granule Cells
M. De Waard, A. Feltz and J. L. Bossu 771
- Activation of a Large-conductance Ca^{2+} -dependent K^{+} Channel by Stimulation of Glutamate Phosphoinositide-coupled Receptors in Cultured Cerebellar Granule Cells
L. Fagni, J. L. Bossu and J. Bockaert 778
- Bypassing the Saccadic Pulse Generator: Possible Control of Head Movement Trajectory by Rat Superior Colliculus
S. M. King, P. Dean and P. Redgrave 790
- Chromatic Discrimination in a Cortically Colour Blind Observer
C. A. Heywood, A. Cowey and F. Newcombe 802
- Single Channel Recording from Glial Cells on the Untreated Surface of the Frog Optic Nerve
H. Marrero, P. M. Orkand, H. Kettenmann and R. K. Orkand 813
- SHORT COMMUNICATION
- Genotypic m3-Muscarinic Receptors Preferentially Inhibit M-currents in DNA-transfected NG108-15 Neuroblastoma × Glioma Hybrid Cells
J. Robbins, M. P. Caulfield, H. Higashida and D. A. Brown 820

The European Journal of Neuroscience

Volume 3 Number 9 September 1, 1991

CONTENTS

RESEARCH PAPERS

- Regeneration of Lesioned Septohippocampal Acetylcholinesterase-positive Axons is Improved by Antibodies Against the Myelin-associated Neurite Growth Inhibitors NI-35/250
D. Cadelli and M. E. Schwab 825
- Paradoxical Modulation of Nociception in Mice by Barbiturate Agonism and Antagonism: Is a GABA Site Involved in Nociception?
J. Carmody, L. Knodler and S. Murray 833
- Loss of Calbindin-28K Immunoreactivity in Hippocampal Slices from Aged Rats: a Role for Calcium?
P. Dutar, B. Potier, Y. Lamour, P. C. Emson and M. C. Senut 839
- Long-term Potentiation of NMDA Receptor-mediated EPSP in Guinea-pig Hippocampal Slices
N. Berretta, F. Berton, R. Bianchi, M. Brunelli, M. Capogna and W. Francesconi 850
- In Vitro* Development of Rat Cerebellar Neurons of Early Embryonic Origin. An Anatomical and Electrophysiological Study
B. Hamon, F. Condé, D. Jaillard, M. Thomasset and F. Crépel 855
- Projections from the Cerebral Cortex to the Red Nucleus of the Guinea-pig. A Retrograde Tracing Study
R. Giuffrida, G. Aicardi and C. Rapisarda 866
- Down-regulation of GAP-43 During Oligodendrocyte Development and Lack of Expression by Astrocytes *In Vivo*: Implications for Macrogial Differentiation
R. Curtis, R. Hardy, R. Reynolds, B. A. Spruce and G. P. Wilkin 876
- C-fos* Induction in the Spinal Cord after Peripheral Nerve Lesion
S. Williams, G. Evan and S. P. Hunt 887
- Distribution of mRNAs for Chromogranins A and B and Secretogranin II in Rat Brain
S. K. Mahata, M. Mahata, J. Marksteiner, G. Sperk, R. Fischer-Colbrie and H. Winkler 895
- Host Brain Regulation of Fetal Locus Coeruleus Neurons Grafted to the Hippocampus in 6-Hydroxydopamine-Treated Rats. An Intracerebral Microdialysis Study
P. Kalén, M. A. Cenci, O. Lindvall and A. Björklund 905

The European Journal of Neuroscience

Volume 3 Number 10 October 1, 1991

CONTENTS

RESEARCH PAPERS

- Transferrin Receptor Expression and Iron Uptake in the Injured and Regenerating Rat Sciatic Nerve
G. Raivich, M. B. Graeber, J. Gehrmann and G. W. Kreutzberg 919
- Effect of Glutamate and Ionomycin on the Release of Arachidonic Acid, Prostaglandins and HETEs from Cultured Neurons and Astrocytes
K. Oomagari, B. Buisson, A. Dumuis, J. Bockaert and J.-P. Pin 928
- Striatal Ascorbate and its Relationship to Dopamine Receptor Stimulation and Motor Activity
T. Zetterström, D. B. Wheeler, M. G. Boutelle and M. Fillenz 940
- The Effects of Activation or Inhibition of the Subthalamic Nucleus on the Metabolic and Electrophysiological Activities Within the Pallidal Complex and Substantia Nigra in the Rat
J. Féger and P. Robledo 947
- Developmentally Regulated Expression of HDNF/NT-3 mRNA in Rat Spinal Cord Motoneurons and Expression of BDNF mRNA in Embryonic Dorsal Root Ganglion
P. Ernfors and H. Persson 953
- L-Homocysteate Preferentially Activates *N*-methyl-D-aspartate Receptors to CA1 Rat Hippocampal Neurons
L. Provini, S. Ito, Y. Ben Ari and E. Cherubini 962
- Lesions of the Cerebral Cortex and Caudate-Putamen Enhance GABA Function in the Rat Superior Colliculus
I. C. Kilpatrick, J. W. Neal, R. C. A. Pearson and T. P. S. Powell 971
- The Effects of NMDA Antagonists on Neuronal Activity in Cat Spinal Cord Evoked by Acute Inflammation in the Knee Joint
H.-G. Schaible, B. D. Grubb, V. Neugebauer and M. Oppmann 981
- The Effect of Calcium Channel Antagonists on Spontaneous and Evoked Epileptiform Activity in the Rat Neocortex *In Vitro*
C. L. Boulton and C. T. O'Shaughnessy 992
- Opposed Behavioural Outputs of Increased Dopamine Transmission in Prefrontocortical and Subcortical Areas: A Role for the Cortical D-1 Dopamine Receptor
P. Vezina, G. Blanc, J. Glowinski and J.-P. Tassin 1001
- Nerve Growth Factor Receptor-immunoreactive Fibres Innervate the Reticular Thalamic Nucleus: Modulation by Nerve Growth Factor Treatment in Neonate, Adult and Aged Rats
M. Fusco, M. Bentivoglio, G. Vantini, D. Guidolin, P. Polato and A. Leon 1008
- Binocular Interactions in the Lateral Suprasylvian Visual Area of Strabismic Cats Following Section of the Corpus Callosum
M. Di Stefano, F. Lepore, M. Ptito, S. Bédard, C. A. Marzi and J. P. Guillemot 1016
- The Isolation and Identification of Spinal Neurons That Control Movement in the *Xenopus* Embryo
N. Dale 1025
- Erratum 1036

The European Journal of Neuroscience

Volume 3 Number 11 November 1, 1991

CONTENTS

RESEARCH PAPERS

- An Organotypic Spinal Cord – Dorsal Root Ganglion—Skeletal Muscle Coculture of Embryonic Rat. I.
The Morphological Correlates of the Spinal Reflex Arc
C. Spenger, U. F. Braschler, J. Streit and H.-R. Lüscher 1037
- An Organotypic Spinal Cord – Dorsal Root Ganglion – Skeletal Muscle Coculture of Embryonic Rat. II.
Functional Evidence for the Formation of Spinal Reflex Arcs *In Vitro*
J. Streit, C. Spenger and H.-R. Lüscher 1054
- Morphological Classification of Bipolar Cells of the Primate Retina
B. B. Boycott and H. Wässle 1069
- The Organization of Projections from Subdivisions of the Auditory Cortex and Thalamus to the Auditory
Sector of the Thalamic Reticular Nucleus in *Galago*
M. Conley, A. C. Kupersmith and I. T. Diamond 1089
- Excitatory Actions of the Metabotropic Excitatory Amino Acid Receptor Agonist, *trans*-(±)-1-amino-
cyclopentane-1,3-dicarboxylate (*t*-ACPD), on Rat Thalamic Neurons *In Vivo*
T. E. Salt and S. A. Eaton 1104
- Dorsal Horn Plasticity Following Re-routing of Peripheral Nerves: Evidence for Tissue-Specific
Neurotrophic Influences from the Periphery
G. R. Lewin and S. B. McMahon 1112
- Axons Sprout and Microtubules Increase After Local Inhibition of RNA Synthesis, and Microtubules
Decrease after Inhibition of Protein Synthesis: A Morphometric Study of Rat Sural Nerves
J. Bustos, J. D. Vial, V. Faúndez and J. Alvarez 1123
- Differential Distribution of Tau Proteins in Developing Cat Cerebral Cortex and Corpus Callosum
B. M. Riederer and G. M. Innocenti 1134
- Ca²⁺ Mobilization in Cultured Rat Cerebellar Cells: Astrocytes are Activated by *t*-ACPD
J. de Barry, A. Ogura and Y. Kudo 1146
- Cytotoxic Effect of Brain Macrophages on Developing Neurons
C. Théry, B. Chamak and M. Mallat 1155
- Facilitation and Delay Sensitivity of Auditory Cortex Neurons in CF – FM Bats, *Rhinolophus rouxi* and
Pteronotus p. parnellii
G. Schuller, W. E. O'Neill and S. Radtke-Schuller 1165
- SHORT COMMUNICATION
- The Gene for Ciliary Neurotrophic Factor (CNTF) Maps to Murine Chromosome 19 and its Expression
is Not Affected in the Hereditary Motoneuron Disease 'Wobbler' of the Mouse
K. Kaupmann, M. Sendtner, K. A. Stöckli and H. Jockusch 1182
- Erratum 1187

**PLEASE NOTE THAT
FROM THE BEGINNING
OF 1992 ONWARDS
THE JOURNAL WILL
ONLY GIVE 50 FREE
OFFPRINTS OF EACH
ARTICLE**

The European Journal of Neuroscience

Volume 3 Number 12 December 1, 1991

CONTENTS

RESEARCH PAPERS

- The Relationship of Microglial Cells to Dying Neurons During Natural Neuronal Cell Death and Axotomy-induced Degeneration of the Rat Retina
S. Thanos 1189
- GABA-Mediated Presynaptic Inhibition in Crayfish Primary Afferents by Non-A, Non-B GABA Receptors
A. El Manira and F. Clarac 1208
- Monosynaptic Interjoint Reflexes and their Central Modulation During Fictive Locomotion in Crayfish
A. El Manira, R. A. DiCaprio, D. Cattaert and F. Clarac 1219
- Topographical Aspects of Intracortical Excitation and Inhibition Contributing to Orientation Specificity in Area 17 of the Cat Visual Cortex
F. Wörgötter and U. T. Eysel 1232
- Long Survival of Retinal Ganglion Cells in the Cat After Selective Crush of the Optic Nerve
L. J. Cottee, T. FitzGibbon, K. Westland and W. Burke 1245
- Organization, Development and Enucleation-induced Alterations in the Visual Callosal Projection of the Hamster: Single Axon Tracing with *Phaseolus vulgaris* Leucoagglutinin and Di-I
S. E. Fish, R. W. Rhoades, C. A. Bennett-Clarke, B. Figley and R. D. Mooney 1255
- Outward Currents in Rat Entorhinal Cortex Stellate Cells Studied with Conventional and Perforated Patch Recordings
C. Eder, E. Ficker, J. Gundel and U. Heinemann 1271
- Aspartate- and Glutamate-like Immunoreactivities in Rat Hippocampal Slices: Depolarization-induced Redistribution and Effects of Precursors
V. Gundersen, O. P. Ottersen and J. Storm-Mathisen 1281
- Activation of AP5-sensitive NMDA Receptors is Not Required to Induce LTP of Synaptic Transmission in the Lateral Perforant Path
C. R. Bramham, N. W. Milgram and B. Srebro 1300
- Localization of Sequences Determining Cell Type Specificity and NGF Responsiveness in the Promoter Region of the Rat Choline Acetyltransferase Gene
C. F. Ibáñez and Håkan Persson 1309
- Complementary Distribution of Calbindin D-28k and Parvalbumin in the Basal Forebrain and Midbrain of the Squirrel Monkey
P.-Y. Côté, A. F. Sadikot and A. Parent 1316
- Serotonin Reinnervation of the Suprachiasmatic Nucleus by Intrahypothalamic Fetal Raphe Transplants, with Special Reference to Possible Influences of the Target
A. Daszuta, C. Marocco and O. Bosler 1330
- The Identification and Localization of the Guanine Nucleotide Binding Protein G₀ in the Auditory System
B. Canlon, V. Homburger and J. Bockaert 1338
- The Distribution of μ and δ Opioid Binding Sites Belonging to a Single Cervical Dorsal Root in the Superficial Dorsal Horn of the Rat Spinal Cord: A Quantitative Autoradiographic Study
D. Besse, M. C. Lombard and J. M. Besson 1343

continued overleaf

Activation of <i>N</i> -methyl-D-aspartate Receptors Induces Endogenous Rhythmic Bursting Activities in Nucleus Tractus Solitarii Neurons: An Intracellular Study on Adult Rat Brainstem Slices F. Tell and A. Jean	1353
SHORT COMMUNICATIONS	
Poor Growth of Mammalian Motor and Sensory Axons Into Intact Proximal Nerve Stumps M. C. Brown, E. R. Lunn and V. H. Perry	1366
Homocysteate, an Excitatory Transmitter Candidate Localized in Glia P. Grandes, K. Q. Do, P. Morino, M. Cuénod and P. Streit	1370
Contents of Volume 3	
Annual author index	
Annual subject index	

Facilitation and Delay Sensitivity of Auditory Cortex Neurons in CF – FM Bats, *Rhinolophus rouxi* and *Pteronotus p. parnellii*

G. Schuller¹, W. E. O'Neill² and S. Radtke-Schuller¹

¹Zoologisches Institute der Ludwig-Maximilians-Universität, Luisenstrasse 14, D-8000 München 2, FRG

²Department of Physiology, University of Rochester, School of Medicine and Dentistry, Rochester, NY 14642, USA

Key words: complex sound, cortical maps, neural computation, horseshoe bat, moustached bat

Abstract

Responses of auditory neurons to complex stimuli were recorded in the dorsal belt region of the auditory cortex of two taxonomically unrelated bat species, *Rhinolophus rouxi* and *Pteronotus parnellii parnellii*, both showing Doppler shift compensation behaviour. As in *P.p.parnellii* (Suga *et al.*, *J. Neurophysiol.*, **49**, 1573–1626, 1983), cortical neurons of *R.rouxi* show facilitated responses to pairs of pure tones or frequency modulations. Best frequencies for the two components lie near the first and second harmonic of the echolocation call but are in most cases not harmonically related. Neurons facilitated by pairs of pure tones show little dependence on the delay between the stimuli, whereas pairs of frequency modulations evoke best facilitated responses at distinct best delays between 1 and 10 ms. Facilitated neurons are found in distinct portions of the dorsal cortical belt region, with a segregation of facilitated neurons responding to pure tones and to frequency modulations. Non-facilitated neurons are found throughout the field. Neurons are topographically aligned with increasing best delays along a rostrocaudal axis. The best delays between 2 and 4 ms are largely overrepresented numerically, and occupy ~56% of the cortical area containing facilitated neurons. A functional interpretation of the large overrepresentation of best delays ~3 ms is proposed. Facilitated neurons are located almost entirely within layer V of the dorsal field.

Introduction

The mammalian auditory cortex is composed of a number of subdivisions or 'fields', whose borders are distinguished both physiologically and morphologically (Woolsey and Walzl, 1941; Brugge and Merzenich, 1973; Merzenich *et al.*, 1975; Reale and Imig, 1980; Suga, 1984). Unfortunately, the functional significance of the various fields has for most species remained relatively obscure. In cats, for example, at least five cortical fields are definable by the presence in each of a complete cochleotopic (tonotopic) map. However, other than a recent report showing that neurons in the anterior auditory field are able to encode higher frequencies of amplitude modulation than neurons in primary field A1 (Schreiner and Urbas, 1988), little further functional differentiation of these apparently redundant representations has been reported.

There is a growing body of evidence from certain species of echolocating bats, especially *Pteronotus parnellii*, showing that different cortical fields may perform distinctly different functions. The moustached bat belongs to an acoustically categorized group called 'long CF/FM' bats. Bats in this group emit pulses which always contain a long-duration constant frequency (CF) component terminated by a downward sweeping frequency modulation (FM), and in some species a number of harmonics.

The auditory cortex of the moustached bat can be subdivided into a

number of functional processing areas (O'Neill and Suga, 1982; Suga *et al.*, 1983a; Suga, 1984). The 'core' region is tonotopically organized following the pattern seen in other mammals, but contains zones where small bands of frequencies are enormously overrepresented (Suga and Jen, 1976; Suga and Manabe, 1982; Asanuma *et al.*, 1983).

Outside this tonotopically organized area, the units have more complex response properties, and show e.g. facilitation to combinations of two or more elements found in the biosonar signal (Suga *et al.*, 1979; Suga *et al.*, 1983a). Units in the 'FM–FM' dorsal fringe and ventral fringe areas are facilitated by, and tuned to, the time interval between pairs of FM sweeps (O'Neill and Suga, 1979; O'Neill and Suga, 1982; Suga and Horikawa, 1986). Areas containing 'FM–FM facilitation neurons' are 'chronotopically' organized to represent these time intervals, thereby forming neural maps of the target range (Suga and O'Neill, 1979; O'Neill and Suga, 1982; Suga and Horikawa, 1986).

Units in the CF/CF cortical field, on the other hand, are facilitated by pairs of near-harmonically related CF signals. The timing between the CF components, as long as they overlap to some extent, is not critical (Suga *et al.*, 1978, 1979, 1983b).

Both types of 'combination-sensitive' neurons are facilitated by pairing

an acoustic component of the first harmonic with one of the higher harmonics in the sonar signal. Neurons facilitated by pairs of elements from the same harmonic are extremely rare (e.g. Suga, 1978). Similar elaborate cortical specializations have been found in other bat species, although single-unit response properties and topographical organization differ from those found in *P.parnellii* (Sullivan, 1982a,b; Wong and Shannon, 1988; Berkowitz and Suga, 1989).

Phylogenetically, the moustached bat (New World family Mormoopidae) and the horseshoe bats (Old World family Rhinolophidae) are not closely related. Behaviorally, however, these species show strong convergence. Both use an unusual biosonar signal (long CF/FM) dominated by narrow-band (CF) elements. Both perform 'Doppler-shift compensation' (Schnitzler, 1968, 1970; Schuller *et al.*, 1974) to stabilize echoes at particular 'reference' frequencies to which their ears are extraordinarily sharply tuned, and both have similar foraging strategies (Link *et al.*, 1986; Belwood and Morris, 1987).

The horseshoe bat cortex is also organized into a 'core-belt' arrangement (Ostwald, 1980, 1984; Schweizer and Radtke, 1980; S. Radtke-Schuller, unpublished). In this study, we have explored the belt areas in the rufous horseshoe bat, *R. rouxi*, to determine whether its cortex shows similarities in organization to the moustached bat. In a companion paper, we examine the anatomical features of the cortical regions in the horseshoe bat which contain these similarly functioning neurons. We compare these results to the relevant regions of the moustached bat cortex, which to date have not been anatomically described. Some of the data have been reported previously (Schuller *et al.*, 1988).

Materials and methods

Five Indian or Sri Lankan rufous horseshoe bats, *R. rouxi*, and five Jamaican moustached bats, *P.p.parnellii*, were used in these studies. Bats were kept in captivity under seminatural conditions for under a year. The animals were surgically prepared under halothane anaesthesia. The skin overlying the skull was additionally infused with local anaesthetic (Novocain). The skin was cut along the midline and reflected to the sides in order to affix, with dental cement, a tube that was attached to the stereotaxic device during experiments. The tube was glued to the caudal part of the skull overlying the inferior colliculi and the cerebellum. Rostral to the fixation tube, the tissue was carefully cleaned from an area of skull ~ 1.5 mm left and right of the midline. This area was used to determine the position of the skull surface in stereotaxic coordinates and to place holes to introduce the recording electrode. After surgery, the animals were allowed to recover through the following day. Throughout the experiments, the wound margins were treated with local anaesthetic (Novocain), but the animals were otherwise unanaesthetized.

The experiments were conducted in an acoustic chamber lined with convoluted foam, which reduces acoustical interference from the environment and minimizes the reflections of ultrasonic signals. The animals were placed in a holder which prevented gross body movements, and the head was immobilized by attaching the surgically affixed tube to a head holder that allowed accurate repositioning (≤ 10 μ m) of the animal in the stereotaxic device throughout the recording series, which lasted for several weeks. The orientation of the brain within the stereotaxic coordinate system was determined by automatically scanning the profile of the exposed skull in both the parasagittal and transverse directions. Details of the stereotaxic device, the procedures to determine the skull position, and the reconstruction of the recording sites are described elsewhere (Schuller *et al.*, 1986). The method yields a typical

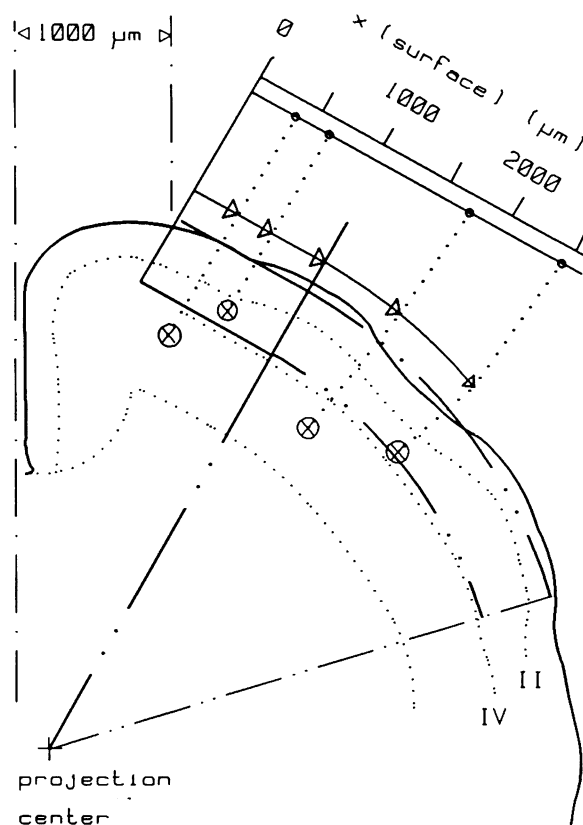


FIG. 1. Surface projection procedure demonstrated on a frontal atlas section. The curvature of layer IV was fitted with straight and circular segments so that the transitions between segments were smooth (i.e. same slope at transition point) and that a good approximation was reached with a minimal number of segments. Location of cells (\otimes) or cytoarchitectural boundaries are projected perpendicularly through the fitted line segments of layer IV, and then to the approximated surface of the cortex. The distance from the origin (arbitrarily fixed at 1000 μ m lateral from the midline of the brain) is straightened out and marked on a line representing the hypothetical flattened cortical surface. Surface projections avoid distance and area distortions due to different curvature of the cortex.

accuracy for the localization of recording sites of 100 μ m in all three dimensions. Localization of the recording sites within the brain was further verified by injection of tracer substances, such as horseradish peroxidase or wheat-germ agglutinin conjugated with horseradish peroxidase, or by making small electrolytic lesions. The measurements of the skull position in stereotaxic coordinates were made during a short (~ 1 h) session on the first postoperative day. The recording experiments started on the second postoperative day with daily sessions no longer than 6 h, which could be repeated over 3 weeks (typically; maximally up to 7 weeks). To prepare the animal for single-unit recording, a small hole was cut into the skull over the target area and the dura was perforated under local anaesthesia. The holes had diameters typically < 500 μ m and several electrode penetrations with different mediolateral inclinations (roughly parallel to the cortical surface) were made through each hole. The positions of the penetrations were all referred to a common reference point, thus allowing a computational reconstruction in coordinates of the respective brain atlases (Radtke-Schuller, unpublished).

For single-unit recording, Parylene-coated tungsten electrodes with impedances between 1.8 and 2.5 M Ω (Micro Probe Inc.) were lowered

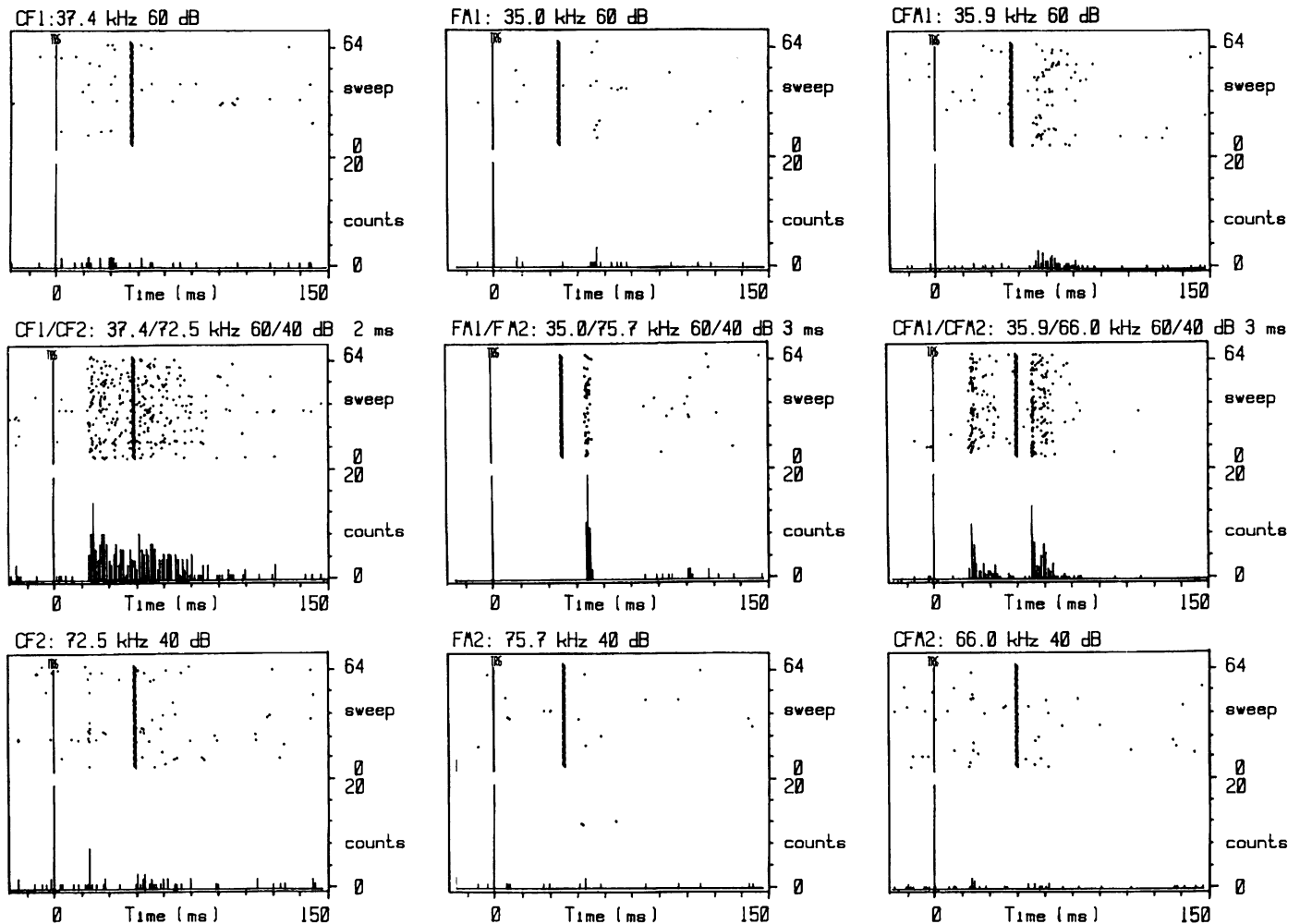


FIG. 2. Representative examples of neurons showing facilitated response to combinations of two stimulus components (frames in the centre row). The responses to either stimulus component alone is represented in the upper (low-frequency component) and lower (high-frequency component) frames. In the left column the combination of two constant-frequency components (CF/CF) elicits facilitated responses. Facilitation by two frequency modulated components (FM-FM) is shown in the centre column. Facilitation by either CF/CF or FM-FM combinations (CFM/CFM or mixed type) is shown on the right. Each frame shows the temporal occurrence of spikes in both a dot display (top) and a peristimulus time histogram (bottom). The onset of the stimulus is delayed by 10 ms with respect to the system trigger (vertical thin lines) and the stimulus ends at the heavy vertical line (shown only in the dot display section). Stimulus type, frequency and amplitude are indicated at the top of each frame.

from the surface of the brain in steps of $2\ \mu\text{m}$, using a piezoelectric micropositioner (Burleigh Inchworm). The exposed electrode tips had diameters of $\sim 1\text{--}2\ \mu\text{m}$ and lengths of $5\text{--}10\ \mu\text{m}$. An indifferent electrode (sharpened tungsten wire) was chronically implanted during the initial surgery in contact with the brain surface under the most anterior part of the skull. The action potentials were amplified, filtered and amplitude-discriminated with conventional methods. The temporal occurrence of spikes was recorded relative to the onset of the acoustic stimuli and could be displayed either as a dot raster or as peristimulus time histograms. Acoustic stimuli with a fixed or a single, stepwise-varying parameter were presented. Each frame, or 'segment', consisted of either 32 or 64 presentations. Recording and processing programs were run on a DEC LSI11/23 computer. All programs were written by M. Betz.

Acoustic stimuli were generated by passing sine waves from function generators (Wavetek) through custom made electronic switches shaping the stimuli into bursts with a 1 ms rise-fall time. Typically, the frequency within the stimulus could be either constant, mimicking the

CF portion of the echolocation call, a linear downward sweep, modelling the final FM portion of the echolocation call, or a combination of both waveforms, forming a CF-FM replica of the echolocation call. Stimulus duration was 28 and 3 ms for the CF and FM components, respectively. Stimuli from two channels could be broadcast together at adjustable interstimulus delays and with independently controlled amplitudes and frequencies. The frequency of each stimulus and the interstimulus time delay could be changed stepwise with different stepwidths during one recording frame, thus allowing an immediate evaluation of frequency- or delay-dependent responses. In addition, harmonically related stimuli, sinusoidally frequency-modulated stimuli and narrow-bandwidth noise stimuli could be presented. The acoustic stimuli were reproduced by a 2 cm diameter electrostatic loudspeaker located 30° contralateral to the recording site and 15 cm away from the bat's ears. The elevation of the loudspeaker was adjusted to place it perpendicular to the plane of the nose leaf (the position of greatest sensitivity of the ear at the reference frequency).

For the determination of the individual resting frequency of the bats,

Figure 2 gives examples of the responses in three different neurons. The activity is represented either in H dot raster displays (where each

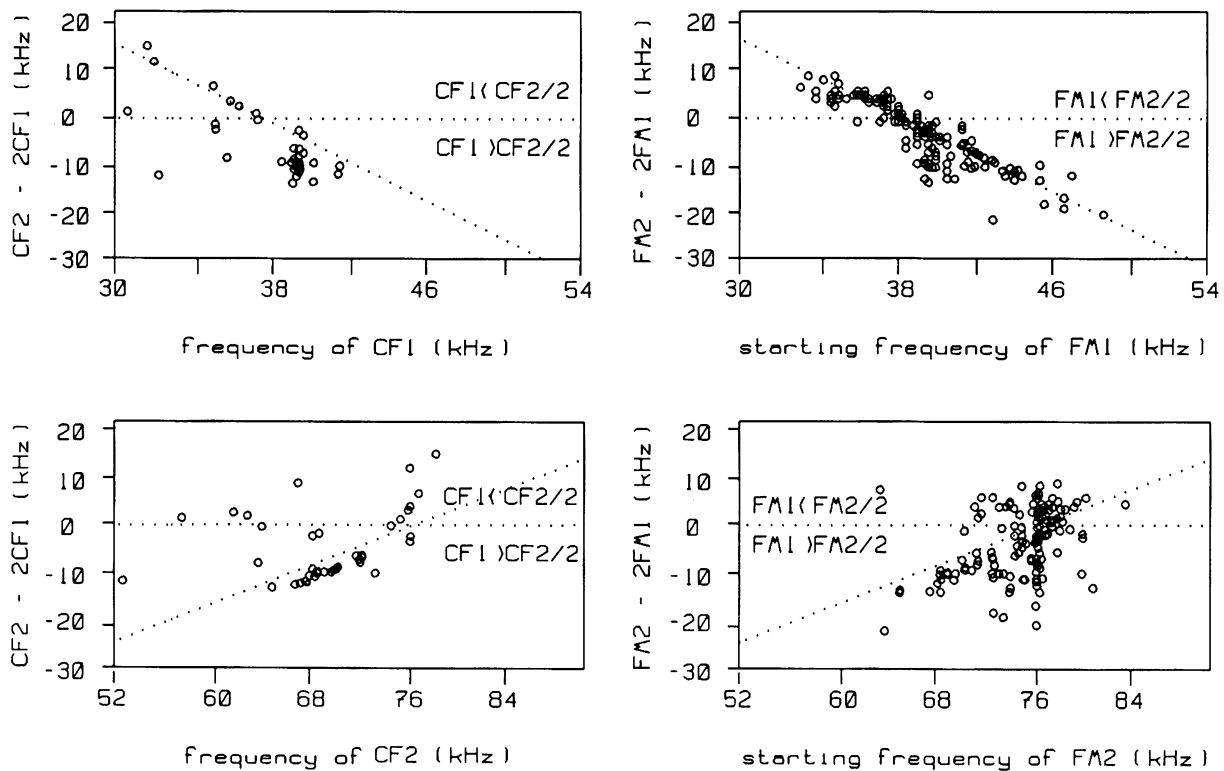


FIG. 4. Relation between best low- and best high-frequency components for facilitation represented as deviation from harmonic relationship ($F2 = 2 \times F1$, ordinate). Negative values mean that the low best frequency was higher or the high best frequency was lower than a harmonic relationship would require. The oblique dotted lines represent the deviations when the upper or lower frequency is kept at resting or half resting frequency, respectively.

dot represents a spike) for several sequences of stimulus presentations, arranged in temporal sequence from bottom to top (upper part of frame), or as a peristimulus time histogram (lower part of frame). The vertical line labelled TRG represents the system trigger, and the stimuli start 10 ms after this trigger. The vertical stack of dashes indicates the end of the stimuli.

The left column of frames shows the responses to CF stimuli: presentation of single CF stimuli at 37.4 or 72.5 kHz alone yielded only little response (upper and lower frame). Coincident stimulation with both CF tones (middle frame) elicited a clear and consistent phasic-tonic response, i.e. distinct facilitation of the response to CF/CF combination tones.

The example in the middle column demonstrates the response properties of a neuron to FM stimuli. The FM components consisted of 10-kHz downward frequency sweeps with 3-ms durations. One FM sweep started at 35.0 kHz and elicited a spike sporadically (upper frame), whereas the other FM sweep, starting from 75.7 kHz, elicited no correlated response at all (lower frame). If the two stimuli were presented together with a temporal delay of 3 ms, they provoked a vigorous response with almost a spike for each presentation. The number of spikes elicited by the combination was by far higher than the sum of activities to the stimuli alone.

In addition to these two types of neurons that were facilitated by either CF/CF or FM-FM combinations, neurons were found that manifested facilitation to both combinations side-by-side. The last column of frames in Figure 2 shows the responses to stimuli termed 'CFM', consisting of a CF followed by an FM (as in the natural echolocation cry). Neither CFM stimulus presented alone (upper and lower frames) elicited much response, but the presentation of the two CFM stimuli with a temporal

delay of 3 ms generated a pronounced response to both the CF and the FM portion (middle frame).

Neurons facilitated by FM-FM combinations were more frequently found (197 out of 247, 87%) than CF/CF facilitated neurons ($n = 23$, 9%) or neurons with the mixed type of facilitation (CFM-CFM, $n = 27$, 11%).

The examples in Figure 2 show neurons with consistent responses over the sequence of stimulus presentations. The excitability in quite a few other cases was less consistent: the unit discharged regularly for periods of time interspersed by periods of little or no response.

All classes of facilitation neurons (CF/CF, FM-FM and CFM-CFM) depended strongly on the spectral content of the components and, especially in FM-FM neurons, on the temporal relationship of the components. If the frequency of one component was kept constant and the frequency of the other, concurrently presented component was swept stepwise through the relevant frequency range, the pattern of discharges mirrored the tuning properties of that frequency component in the particular stimulus constellation. Figure 3 shows the tuning properties for the CF/CF, FM-FM and CFM-CFM neurons in Figure 2 (from left to right). In the upper row the high-frequency component was fixed and the low-frequency component was incremented in 64 equidistant steps from 25, 25 and 20 kHz to 55, 45 and 60 kHz, respectively. The CF/CF neuron (top left column) was clearly facilitated when the frequency of the lower CF component was between 34 and 46 kHz. The FM-FM neuron (middle) showed much sharper frequency tuning between 34 and 38 kHz (initial frequency of the FM sweep) for the lower FM component. Interestingly, the neuron that exhibited facilitation to both CF and FM pairs (right) responded over different frequency ranges for the two components, i.e. 28–34 kHz for the CF

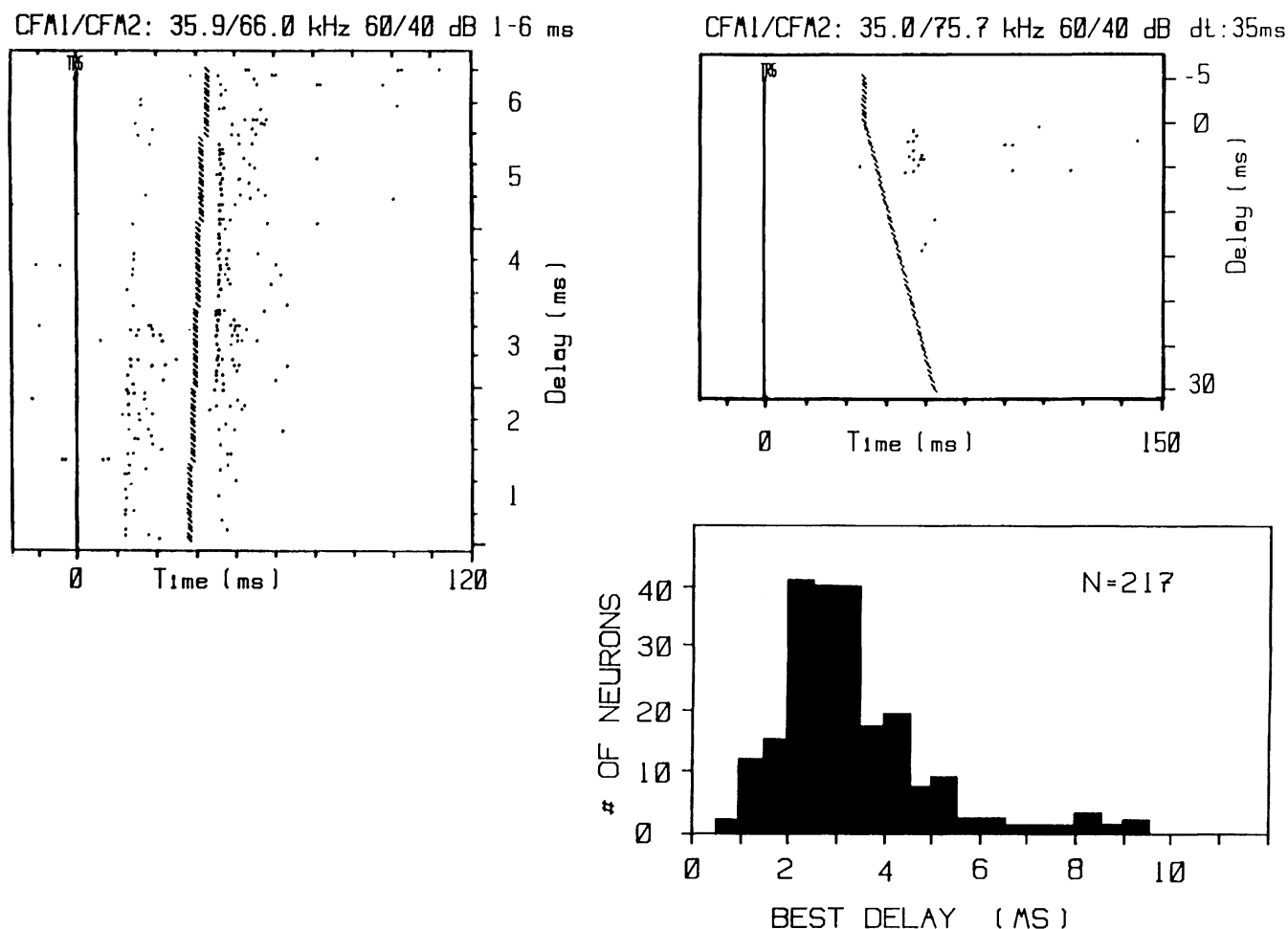


FIG. 5. Delay dependence of facilitated responses. The delay tuning is represented in the two upper graphs, in which the temporal delay of the high-frequency component is changed stepwise between 1 and 6 ms or between 30 and -5 ms, respectively. Note that the response to CF/CF components also shows delay-dependent facilitation. The histogram (bottom right) gives the distribution of best delays of FM-FM neurons and shows the overrepresentation of neurons with best delays between 2 and 4 ms.

and 30–42 kHz for the FM. Similar results were obtained when the frequency of the lower component was fixed while that of the upper component was varied (lower row). The tuning ranges were generally much narrower for both the CF/CF and FM-FM neurons: 72–72.6 kHz and 71.5–76 kHz, respectively. In the CFM-CFM neuron the tuning range was broad for the upper component, ranging from about 60 to 72 kHz. For the high-frequency component there was no discernible difference between CF and FM tuning ranges, like that seen for the low-frequency component.

The details of frequency tuning for facilitation depend on the choice of frequency of the upper (high-frequency) component. In order to determine the best frequencies for the two components yielding the optimal facilitated response, the best facilitation frequency (BFF) of the high-frequency component was determined first because of its much narrower tuning. Then, keeping the high-frequency component constant (at BFF), the low-frequency component was stepped through the relevant frequency range to determine its BFF. In neurons with FM-FM facilitation, the temporal delay that gave best responses (see below) was held constant as well.

The relationship between the two BFF's was in most cases not harmonic, i.e. the lower BFF was not equal to half the upper BFF. Figure 4 represents deviation from the harmonic interval as a function of the

frequency of the upper BFF for CF/CF (left) and FM-FM (right) neurons. All frequencies have been normalized to a standard resting frequency of 76 kHz in order to allow comparison of the data across bats. This was done by subtracting the individual bat's resting frequency from all frequency values in recordings from this bat, and subsequently adding 76 kHz to standardize the resting frequency. The ordinate gives the difference between upper BFF (CF2 or FM2) and twice the low BFF (CF1 or FM1). Positive values above the dotted horizontal line indicate that the lower BFF was below the harmonic interval, and vice versa. The oblique dotted line gives the locus of 76 kHz BFFs in the upper graphs, and of 38 kHz BFFs in the lower graphs.

One can discern several interesting features of CF/CF neurons from the graphs in the first column. There was a clear preponderance of neurons with lower BFFs slightly above 38 kHz, and up to 12 kHz above the harmonic interval for the upper BFF. In the lower graphs it is also apparent that only a minor fraction of CF/CF neurons had high BFFs at, or slightly above, the normalized resting frequency of 76 kHz. The harmonic deviation of 74 % of the neurons is negative, meaning that the lower BFF was higher than the harmonic interval determined by the upper BFF. Alternatively, the upper BFF was less than the ideal harmonic interval specified by the lower BFF.

For FM-FM neurons the situation was somewhat different, in that

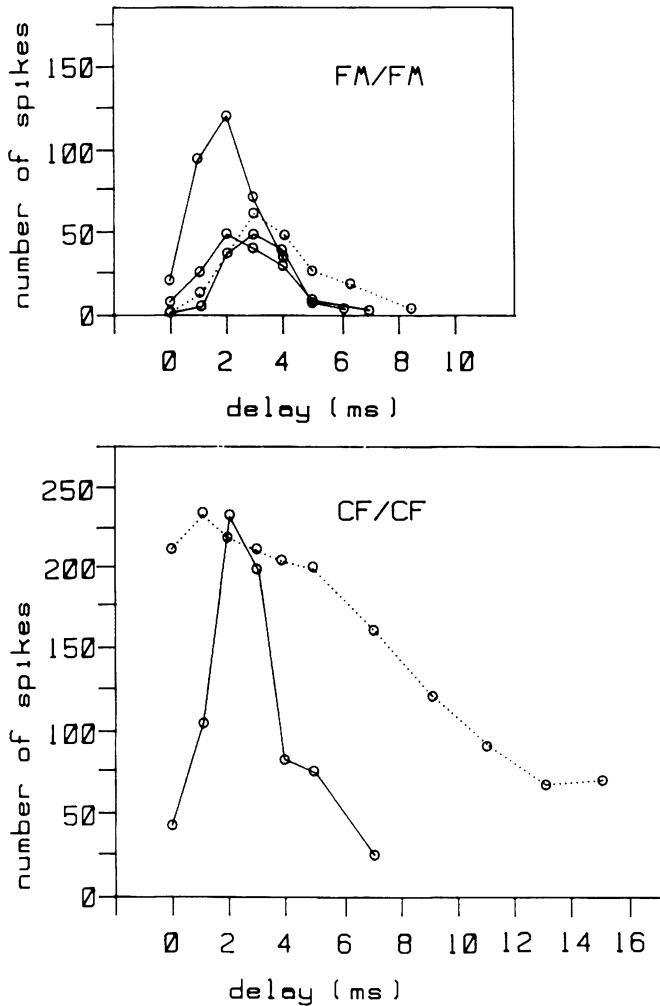


FIG. 6. Delay tuning curves for FM-FM- and CF/CF-facilitated neurons. The examples in the upper graph show the most commonly found delay tuning properties in FM-FM neurons, whereas those in the lower graph exemplify only a minority of delay-dependent CF/CF neurons, most of which were much less sharply tuned than those shown.

the BFF of the higher component clustered at, or slightly above, the resting frequency. This is indicated by the accumulation of neurons along the oblique dotted line in the upper right graph, and at and above the 76 kHz abscissa value in the lower graph. For the lower BFF, a cluster of neurons at ~ 39 kHz can be discerned. Also, in FM-FM-facilitated neurons there was a tendency for the deviation from harmonic relation to be preponderantly negative, i.e. the lower BFF was most often higher, or the upper BFF lower, than a harmonic relation would dictate.

The optimal stimulus intensities for the two components were not systematically investigated, but the typical best sound pressure levels for the low-frequency component were between 40 and 80 dB SPL, and for the high-frequency component between 10 and 50 dB SPL. Facilitated responses were best if the difference between the two components was between 10 and 30 dB.

The latencies of the responses to single stimuli as well as to combinations varied widely (4–30 ms), most falling between 10 and 15 ms. The minimal latencies ranged between 4 and 7 ms.

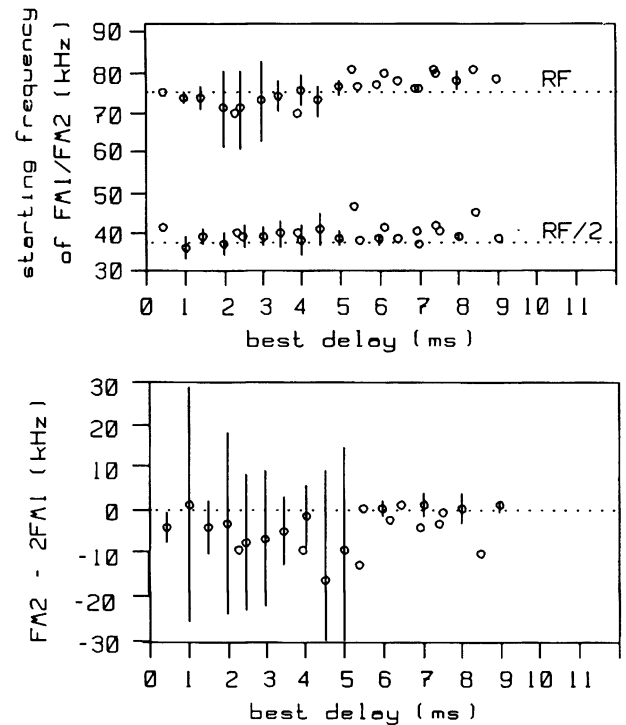


FIG. 7. (Top) Mean best frequencies for high and low frequency components of FM-FM neurons versus their best delays. (Bottom) Difference between upper and twice the lower BFFs versus best delay. The bars represent standard deviations where applicable. Note the increasing deviations from a strict harmonic relationship for best delays of < 5 ms depicted in the lower graph.

Dependence on time delay

In all neurons facilitated by FM-FM combinations, the facilitation was clearly a function of the temporal delay between the low- and the high-frequency component. The responses to a sequence of stepwise increases of the temporal delay are shown for a CFM-CFM neuron in the left graph of Figure 5. Only a few spikes were elicited in response to the final FM-FM combination at delays of 1 and 2 ms (bottom). When the two FM portions were separated by 3–5 ms, the cell fired consistently and vigorously. Beyond that, only a few spikes were elicited when the delay increased to 6 ms (top). Even longer delays (not shown) gave no response at all. The delay tuning of another FM-FM neuron is given in the upper right graph of Figure 5, where the delay was swept over 35 ms starting from 30 ms (bottom) and ending at -5 ms (top). The neuron discharged consistently at delays between 1 and 4 ms to the later of the two FM components.

The best delays, i.e. the temporal delays yielding the optimal facilitation, of 217 units were distributed over a range from 0.5 to 9.5 ms with a clear overrepresentation of the 2–4-ms delay range. Long best delays above 6 ms were very rarely encountered, comprising only 5% of the sample of facilitated neurons. This scarcity of long best delays is not merely a sampling error, as will be seen later on in this paper.

Not only were FM-FM neurons sensitive to temporal delays, but also the CF/CF-response of CF/CF or mixed d-type neurons showed delay sensitivity. This can be seen in the left dot display in Figure 5, which shows increased response by a mixed d-type cell to the CF components at 2 ms delay, compared to the responses at 1 ms or > 3 ms delays.

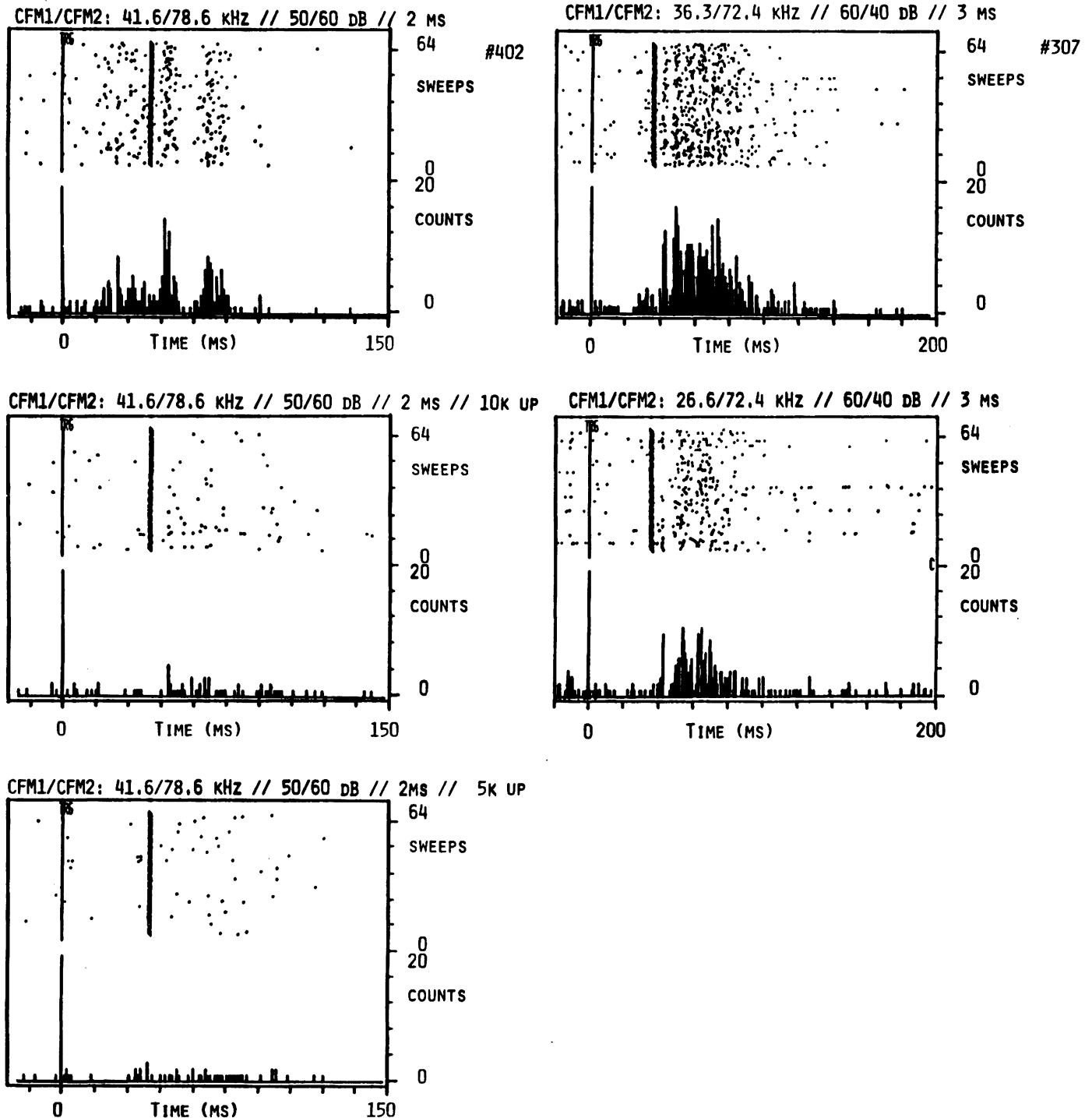


FIG. 8. (Left) Responses to combinations of CFM components (upper frame) and the same combination with the addition of an initial upward frequency sweep of 10 kHz (middle) or 5 kHz (lower frame) to the high-frequency component. The addition of the initial FM portions almost completely abolishes the facilitated response. (Right) Reversal of the direction of the final frequency sweep of the lower frequency component. The facilitated response is reduced.

Examples of discharge magnitude-versus-delay functions are given in Figure 6 for FM–FM neurons (upper graph) and for CF/CF neurons (lower graph). The temporal bandwidth is roughly the same for FM–FM neurons with best delays of 2–4 ms, amounting to between 2 and 3 ms at 50% maximal activity. Delay tuning in CF/CF neurons could be either

absent, show a preference for short delays ('low-pass', dotted curve), or be selective for a distinct range of delays ('bandpass', solid line).

Delay tuning of facilitated neurons was also affected by the frequencies (or bandwidths) of the two stimuli. Different combinations induced shifts in the best delay of up to 1 ms, so that the best delay is only characteristic

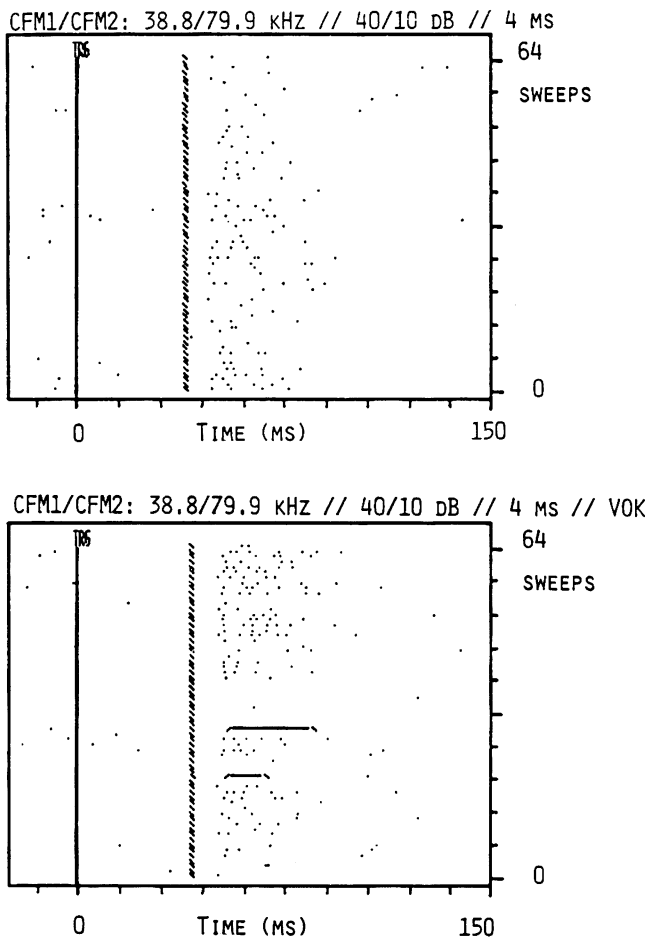


FIG. 9. Influence of vocalization on the response of neurons showing facilitation to CFM/CFM combination stimuli. The upper graph shows the neuronal response without vocalization. The spontaneously emitted vocalizations during the recording in the lower graph lead to a complete suppression of the response for 4–10 subsequent stimulus presentations. Vocalizations are indicated by horizontal bars in the dot display; the temporal sequence of stimulus presentation is from bottom to top.

for a neuron at particular frequencies of the facilitating components. The relationship between the best delays and the mean BFFs for FM–FM neurons is represented in Figure 7. The lower BFF was usually slightly higher than half the resting frequency, whereas the upper BFF had, on the average, a minimum at best delays of 2 ms. At shorter and longer delays, the mean upper BFFs approached and exceeded the normalized resting frequency at 76 kHz. The lower graph in the Figure presents deviations from the harmonic interval between the components. It is striking that, on average, it was negative for the most common best delays for facilitation, although the standard deviations were large. In other words, either the low-frequency component is generally higher, or the high-frequency component lower, than a harmonic interval.

Influence of an initial FM sweep on facilitation

Some rarely encountered neurons were recorded which had interesting properties. Figure 8 summarizes the influence of an initial upward frequency sweep (left frames) and of the direction (downward or upward) of the final FM sweep on the facilitated response of one such cell. The upper dot display on the left shows the facilitation of the neuron when

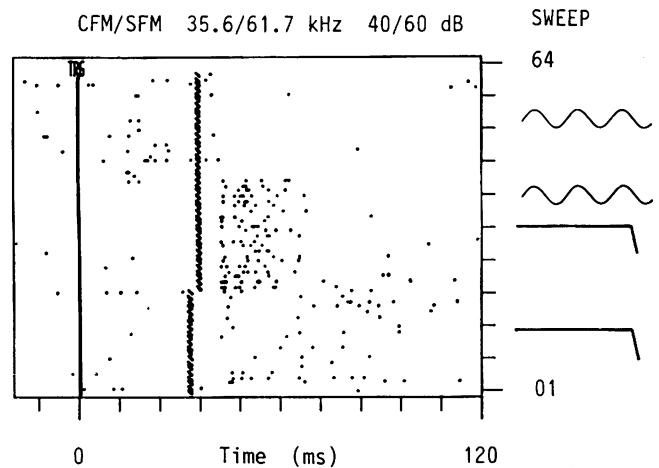


FIG. 10. Facilitated responses to FM/SFM combinations. The graph shows the responses to the sinusoidally frequency-modulated component (SFM, top) or to the lower CFM component alone (bottom). The strong facilitated response to the combined presentation (middle) shows the independence of facilitation from the waveform of the frequency sweep.

stimulated with a pair of CFM stimuli. Both CF/CF and FM–FM facilitation can be seen in the stimulus constellation given at top of the frame. The activity elicited when the single components were presented alone was minimal. When under otherwise identical conditions an initial upward frequency sweep of 10 kHz (middle) or 5 kHz (lower frame) was added to the high-frequency component, the facilitation vanished, leaving only weak and inconsistent activity after the stimuli. The facilitation by the CF/CF pairing seems to be more completely abolished than that caused by the FM–FM. The influence of initial frequency sweeps was demonstrated in only three neurons, but was not routinely examined during these experiments. Therefore no general statement about this interesting effect can be made at this time.

Influence of FM sweep direction on facilitation

On the right side of Figure 8 the influence on facilitation of sweep direction of the terminal FM in the lower component is shown. The upper frame shows the facilitated FM–FM response in the common situation in which both frequency sweeps drive downwards. The response was pronounced and well above the response to single components. When the low frequency component was swept upward (reversed) over the same frequency band, the facilitated response was reduced, but showed the same discharge pattern (lower frame). Changes in the number of spikes but not in discharge pattern were found in the facilitated response of FM–FM neurons upon reversal of the sweep in the low-frequency component.

Influence of duration

Four CF/CF neurons showed an interesting phenomenon in that they responded to combinations of the CF components when the lower frequency component was considerably reduced in duration. As little as 1–2 ms duration of this component was sufficient to induce the full facilitated response.

Effects of vocalization on facilitation

Spontaneous vocalization of the bat typically had marked influences on the response of facilitated neurons. In almost all facilitated neurons, vocalizations emitted during recording led to a shutdown of the response.

Figure 9 shows an example of a neuron which displayed consistent facilitation to FM–FM combination stimuli. When spontaneous vocalization occurred (indicated in the lower frame by horizontal bars) the neuron became completely silent for the next few stimulus presentations (i.e. those above the bar). In the few neurons recorded concurrently with vocalizations ($n = 5$) this blanking effect was always found.

Another interesting response was found in two neurons which were stimulated with either a CFM stimulus (consisting of a CF at 35.6 kHz and a terminal 5-kHz downward sweep), a sinusoidally frequency-modulated stimulus (modulation depth 5 kHz, modulation frequency 100 Hz) with a carrier frequency of 65 kHz, or a combination of both stimuli. Figure 10 shows that neither of the stimuli alone elicited consistent activity (upper and lower region of the raster display), whereas the combination produced vigorous discharge of the neuron (middle) after the end of the stimuli. The response is similar to that evoked by conventional FM–FM combinations. Evidently, the final transient of

the sinusoidal frequency modulation mimics the facilitation caused by the high-frequency FM component.

Topographical organization of facilitated neurons

Neurons with facilitated responses to CF or FM combination stimuli were only found in the dorsal areas of the auditory cortex in the horseshoe bat. Figure 11 shows the forebrain of the bat both from the side and from above, showing the part of the cortex which was flattened following the procedure described in the methods to represent the physiological data in a normalized form. The corresponding boundaries make up the frames for the graphs accompanying the overview, which represents the distribution of all facilitated and non-facilitated neurons recorded in this investigation. The neurons exhibiting facilitated responses are concentrated in a 500–1500- μm -wide dorsal belt and cover a rostrocaudal distance up to 1650 μm . This cortical area is not exclusively occupied by facilitated neurons, as neurons showing no specialization to combination stimuli are found there in considerable numbers (lower

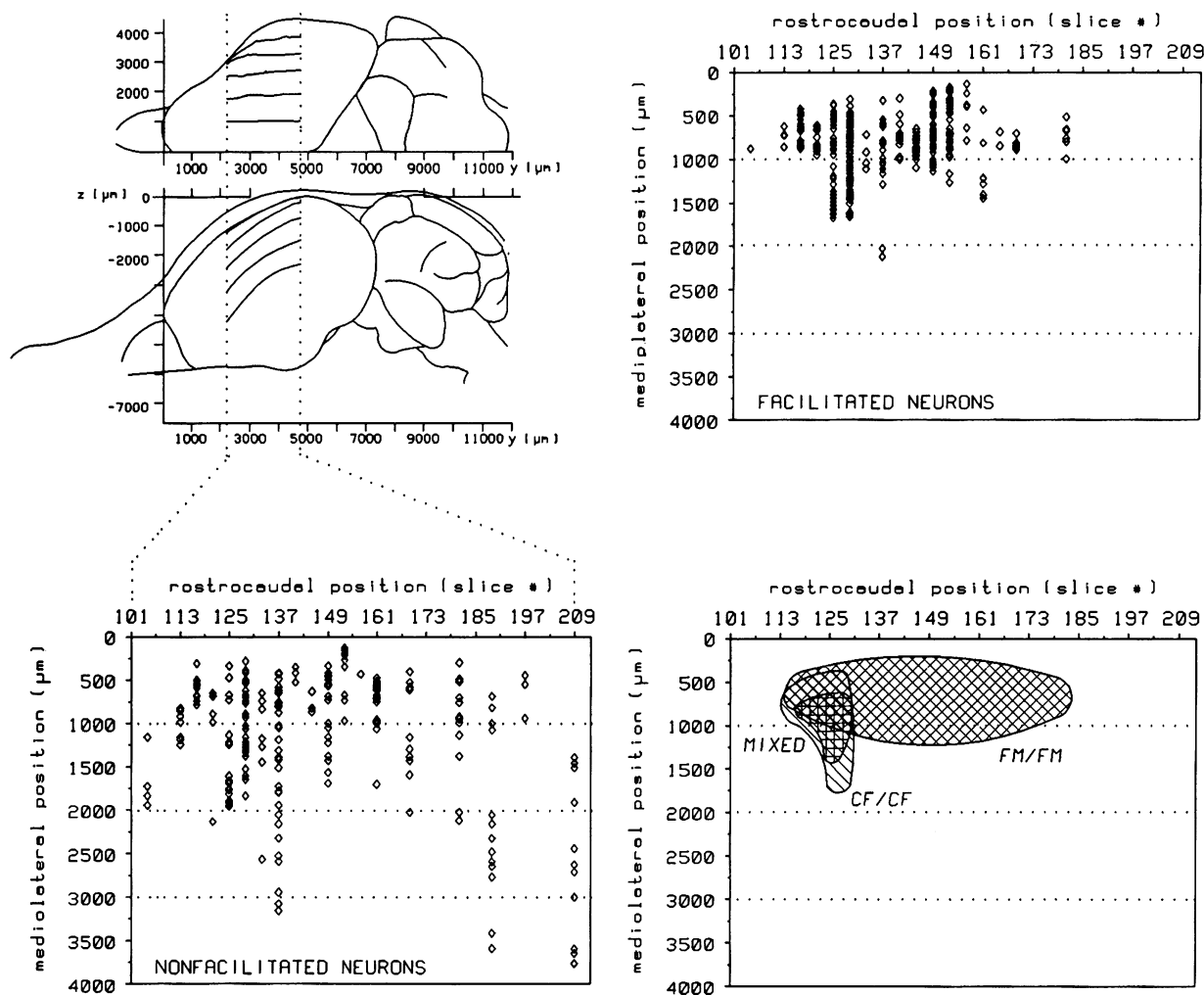


FIG. 11. Topographical distribution of neurons on the cortical surface. The locations of recordings are projected on the cortical surface following the method described in Figure 1 and are represented for the rostrocaudal positions from slice 101 to slice 209 and for a lateral span of 4000 μm , starting at the lateral reference coordinate at 1000 μm . The position of this cortical area is indicated in the upper left graph, which shows the skull profile and brain from the top (upper drawing) and side (lower drawing). Due to the cortical curvature the lateral isodistance lines (connecting points equidistant from the midline) are not straight in these views. The lower left panel shows the locations where neurons could be found that were not facilitated by the combination stimuli (non-facilitated neurons). The locations of facilitated neurons are shown in the upper right panel. The cartoon-like graph at the lower right outlines the areas where specific types of facilitated responses primarily occur. In the rostral part of the dorsal field clear-cut segregation of the different facilitation types could not be found.

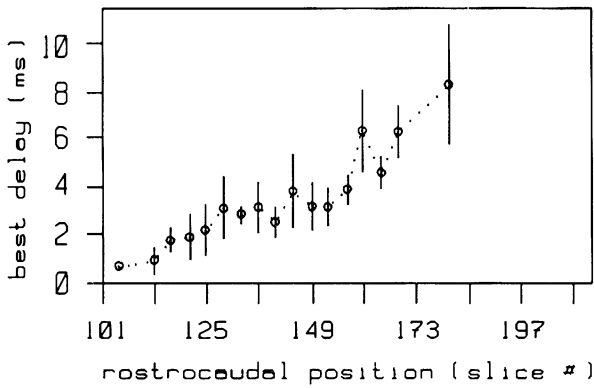


FIG. 12. Rostrocaudal position of FM-FM facilitated neurons with distinct best delays. The mean best delays are represented with their standard deviations. The most important aspect of this curve is the spatial overrepresentation of best delays around 3 ms.

graph). Within the cortical field, the stimulus combination producing facilitation is regionally distinct (Figure 11, lower right). The caudal two-thirds of the field (slices 137–181; slices are $22\ \mu\text{m}$ apart) contained neurons facilitated exclusively by FM-FM combinations. FM-FM neurons were also found in the dorsalmost part of the rostral third of the field. CF/CF facilitation occurred rostrally (slices 113–133), where the facilitated cells are mainly located laterally ($750\text{--}1750\ \mu\text{m}$ mediolateral position). CFM-CFM neurons, facilitated by both stimulus combinations, are concentrated at the same rostrocaudal levels, but slightly more dorsal than CF/CF neurons.

The best delay of FM-FM neurons varied systematically in the rostrocaudal direction. The means and standard deviations of best delays as a function of the rostrocaudal position within the dorsal field are shown in Figure 12. Best delay increases steadily from $<1\ \text{ms}$ rostrally (slice 105) to $3\ \text{ms}$ (slice 129). It then remains constant for $\sim 600\ \mu\text{m}$ (slices 129–157), a region comprising 40% of the rostrocaudal extent of the field, before increasing again caudal to slice 157. Therefore, the topographical arrangement for neurons with distinct best delays is not

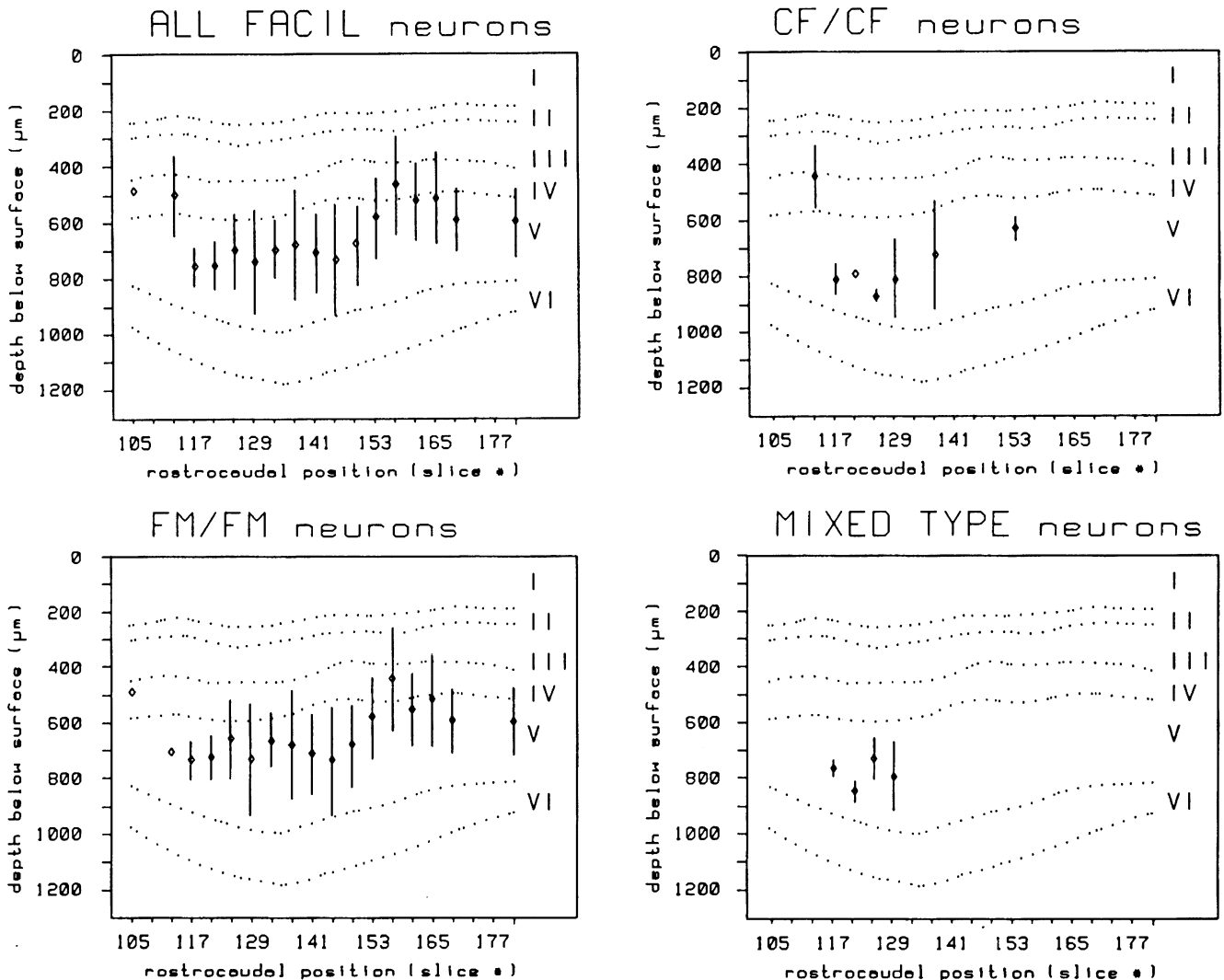


FIG. 13. Location of facilitated neurons within cortical layers. The mean depth below cortical surface of recordings (filled circles) with standard deviations (bars) are given for rostrocaudal positions covering the dorsal field. The dotted lines indicate the ventral borders of the cortical layers noted to the right. Distinct types of facilitated neurons show differences in location within cortical layers.

linear with distance in the plane of the cortex: neurons with best delays ~ 3 ms are not only overrepresented numerically, but they also occupy a much larger cortical area than neurons with shorter or longer best delays. Caudal to slice 157 the recording probability for facilitated neurons sharply decreased, and few neurons with best delays > 6 ms were found.

Depth of recordings

Recordings of neurons were in general restricted to distinct depths below the cortical surface. Facilitated responses were only found between 400 and 800 μm , with a clear concentration ~ 700 μm . No facilitated responses could be located outside this range and certainly did not occur throughout an entire cortical column (Figure 13, upper left). The boundaries of the layers (stippled lines) are given as mean depth values of the cytoarchitectonic borders over a 1000–3000- μm lateral extent of the unrolled cortex. The bulk of facilitated neurons was concentrated in layer V, and encroached on the bottom of layer IV in more caudal recording sites. CF/CF and mixed type neurons (Figure 13, right) were

more commonly found 100 μm deeper in layer V than FM–FM neurons (Figure 13, lower left).

The sequence of neurons responding to either component alone (FM1 or FM2) and to the combination of the two components was stereotyped in many penetrations. When lowering the electrode in a dorsal approach, neurons activated by the FM1 component alone were encountered first, followed by facilitated cells responding to the combination stimulus, and still more ventrally neurons driven by the FM2 component prevailed. It thus appears that there is a layer-specific arrangement of response types in this part of cortex.

Moustached bat

The stereotaxic recordings in the dorsal field of the moustached bats were primarily conducted to define the boundaries of the fields with facilitated responses, with exactly the same procedures used in the horseshoe bat. This enabled comparison of the fields between the two species physiologically and anatomically based on the brain atlases available for both (S. Radtke-Schuller, unpublished).

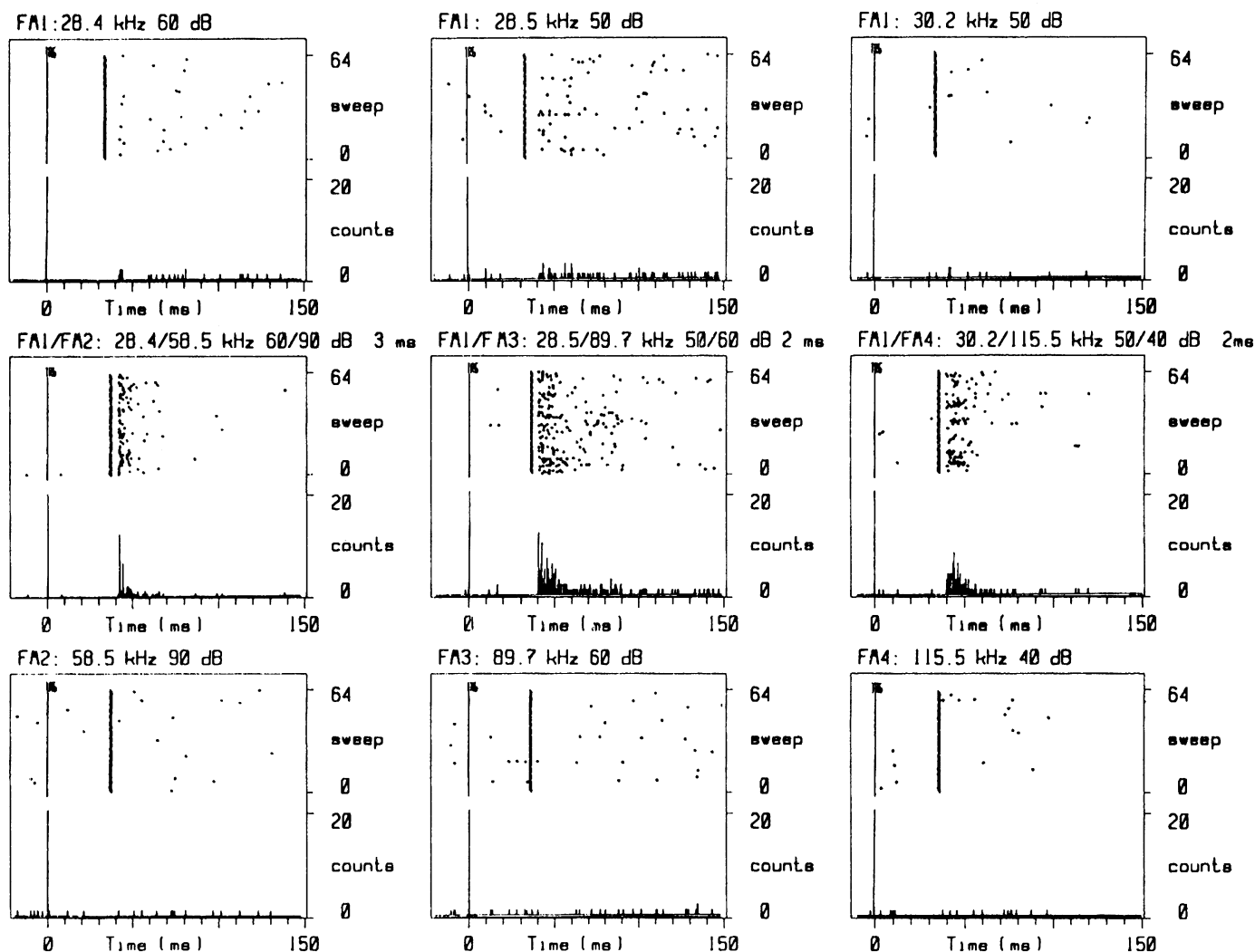


FIG. 14. Representative examples of neurons showing facilitated responses to combinations of two frequency-modulated (FM) stimulus components in *Pteronotus p. parvelli*. The responses to either stimulus component alone are represented in the upper row (low-frequency component, FM1) and lower row (high-frequency component, FM2, FM3, FM4, respectively). The activity elicited by a FM1–FM2 combination (left column), FM1–FM3 combination (middle column) or a FM1–FM4 combination (right column) is shown in the frames of the middle row. Stimulus type, frequency, amplitude and delay are indicated at the top of each frame.

The spike activity of a total of 195 neurons was monitored in the dorsal areas of the auditory cortex in five bats. Sixty-six per cent (117) of the neurons were facilitated by FM–FM combinations, while 6% (12) were facilitated by CF/CF. Within the class of FM–FM facilitated neurons, 36 were sensitive to a combination of the first harmonic (FM1) and the second harmonic (FM2) (Figure 14, left column), 51 responded to FM1 and the third harmonic (FM3) (Fig. 14, middle column) and 30 to a combination of FM1 and the fourth harmonic (FM4) (Fig. 14, right column). Especially in FM1/FM4 neurons, the responses showed variations in strength on successive stimulation sweeps. Periods of vigorous responses were followed by near-silent periods, and the modulation of activity appeared to be cyclic.

The few CF/CF neurons recorded (12) all responded to a combination of the first and third harmonics. In Figure 15 (left column) an example is represented in which the neuron was not activated by the lower harmonic (CF1) component (top), not totally silent to the upper harmonic (CF3) component (bottom), but showed clearly facilitated responses when both components were presented together (middle).

Mixed type neurons showing facilitation to both CF/CF and FM–FM combinations were also found, the type of facilitation dependent on the frequency of the upper harmonic. Figure 15 (right column) shows such a mixed type neuron. It exhibited clear CF/CF facilitation for frequencies of the upper harmonic between 86 and 89 kHz and showed FM-FM facilitation between 87 and 98 kHz. Fewer mixed type neurons were

found in *Pteronotus* (3) than in *Rhinolophus*, which might partly be due to the smaller sample of neurons in this species.

The tuning properties of the facilitated responses for the different components in FM–FM neurons is represented in Figure 16. The starting frequency of FM stimuli is indicated in each case. The spike trains shown in the dot rasters are elicited by stimuli with stepwise increasing frequencies of one component (ordinate), while the frequency of the other component was kept constant. The upper row shows the responses when the fundamental frequency ($f(\text{FM1})$) was varied while keeping the higher harmonics (FM2 (left), FM3 (middle), FM4 (right)) constant at the respective best frequency for facilitation. In the lower row the FM1 component is fixed at best frequency and the frequency of the upper components (FM2, FM3, FM4) is swept through the relevant range.

The most striking tuning property is that the facilitating frequency bands almost always lie below the respective harmonics of the normalized echolocation calls of the individual bats (30.5, 61, 91.5 and 122 kHz). This is again visible in Figure 17, which compiles data on the relationship of best facilitating frequencies in FM–FM neurons. Most BFFs are below the respective harmonics (abscissa) of the echolocation calls. The ordinate gives a measure of the harmonic deviation. When the two facilitating components are harmonically related, data points would lie on the horizontal line. The majority of neurons show negative values, meaning that the upper component has a lower best frequency than a harmonic relationship would require.

Other general response properties corresponded to those described in detail by O'Neill and Suga (1979, 1982), Suga and O'Neill (1979) and Suga *et al.* (1983a). There were some differences in the response properties in the two species, in that the neurons in the moustached bat generally responded more briskly and consistently than those in the horseshoe bat, even though the recording procedures and the electrodes used were identical. The same was true for the facilitated response, in that the facilitation was generally more pronounced in the moustached bat, i.e. more units exclusively responding to combinations were found than in the horseshoe bat.

The dependence of facilitation on the time delay between the two FM components is represented for two neurons in Figure 18A. At delays shorter or larger than the best delay (2 ms in both examples) the spike rate typically decreased rapidly (within a few milliseconds) to baseline level. The results of rate–delay functions in this study conform to previously published material on the moustached bat.

In our recordings, only very few neurons were found that responded to FM–FM combinations with long delays (maximal best delay was 7 ms). The vast majority of neurons had best delays between 2 and 4 ms. Figure 18B gives the best delay distributions for the three different FM1–FM n combinations. Only FM1-FM4 neurons showed higher best delays forming a second peak in the distribution at 5–6 ms.

The numerical overrepresentation of the best delays ~ 3 ms corresponds well to that found in the horseshoe bat. The cortical areas with facilitated neurons were systematically scanned beyond their borders, indicated by the lack of facilitation by combination stimuli and/or the presence of pure tone-driven neurons. Therefore, this prevalence of best delays ~ 3 ms cannot be interpreted as a mere consequence of repeated sampling in the same areas; it represents an enlarged cortical volume specific to this range of best delays.

Despite the use of an accurate stereotaxic approach we could not reproduce clearly the gradients of best delays along the rostrocaudal axis with penetrations in frontal planes. This was also the case in early experiments exploring functional organization in the moustached bat cortex in a different laboratory. It seems that the demonstration of this

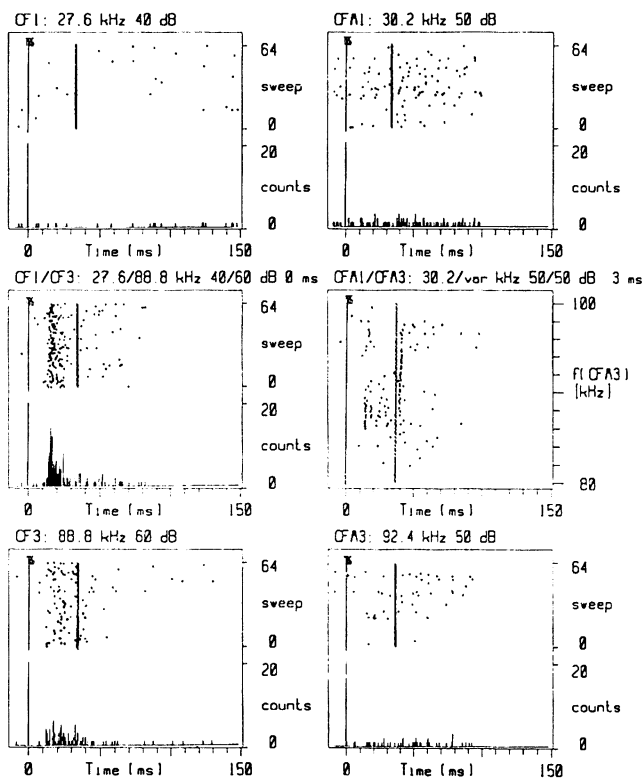


FIG. 15. Responses of facilitated neurons in *Pteronotus p. pamellii* to CF1/CF3 (left column) and CFM1/CFM3 combination stimuli (mixed-type response, right column). The upper and lower frames show the activity elicited by the stimulus components alone, and the middle frames give the discharge pattern to the stimulus combinations. In the mixed-type neuron (right column, middle) the frequency of the CFM3 component has been raised stepwise from 80 to 100 kHz. Stimulus type, frequency, amplitude and delay are indicated at the top of each frame.

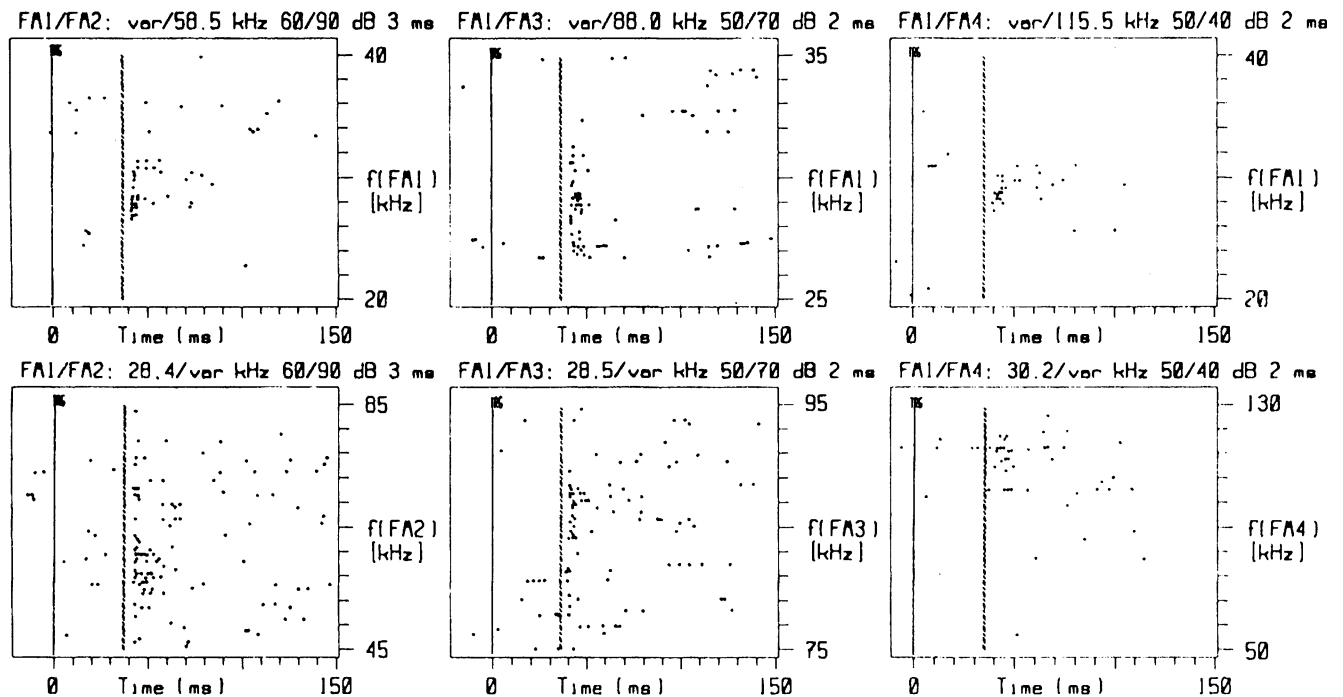


FIG. 16. Frequency dependence of facilitation for FM1–FM2 (left), FM1–FM3 (centre) and FM1/FM4 neurons (right) in *Pteronotus p. parnellii*. The frequency of one component was swept stepwise through the frequency range indicated by the scale on the right side of each frame, whereas the frequency of the other component was kept constant (upper row, lower-frequency component varied, lower row, high-frequency component varied). Fixed parameters are printed at the top of each frame. The dot patterns indicate at which frequencies facilitated responses occurred. The same neurons as in Figure 14 are represented.

topographical arrangement necessitates a rostrocaudal path of penetration following this gradient.

Discussion

Pattern of echolocation calls

The two bat species, *R. rouxi* and *P. parnellii*, use very similar echolocation calls, consisting of long-duration (tens of milliseconds) constant frequency components terminated by short (~ 3 ms), downward frequency sweeps. The initial upward frequency sweep is not ubiquitous in the horseshoe bat signal, varying greatly in intensity and sweep range (Neuweiler *et al.*, 1987). The most important difference between the two echolocation signals is in their harmonic composition. In the moustached bat, the call contains up to five harmonics (fundamental frequency ~ 30 kHz), whereas in the horseshoe bat the call contains only two (fundamental ~ 38 kHz).

Facilitated responses in the horseshoe bat are in accordance with the simple structure of its signal, in that only combinations of the fundamental and the second harmonic produce such responses. No other combinations, e.g. two second-harmonic components, have facilitating effects in cortical neurons within the area where we recorded (Fig. 11). In this way the response properties of the horseshoe bat's dorsal cortical field agree fully with those in the moustached bat's dorsal cortical field.

These two bat species are members of unrelated taxonomic families, and therefore might have evolved the specificity for different harmonic combinations independently. On the other hand, facilitated responses to FM–FM combinations are not unique to CF/FM bats. In the FM bat *Myotis lucifugus*, the facilitating combination is not composed of harmonically related, lower and upper frequency components. Rather,

two FM1 components, mimicking pulse and temporally shifted echo, facilitate the response in cortical neurons (Sullivan, 1982a,b; Berkowitz and Suga, 1989). The facilitation is maximal if the earlier pulse component is of greater amplitude and higher in frequency by several kHz than the delayed echo.

Even though the frequencies of the two components are only a few kHz apart in the latter case, versus widely spaced in the two CF/FM bats, there might be a common neuronal mechanism, distinguished only quantitatively. Thus the combination sensitivity of these cortical neurons might be a rather general feature, with the precise frequency ranges selected for conjoint processing adapted to unknown behavioural demands.

Self-stimulation by vocalization

Pietsch and Schuller (1987) have shown with cochlear microphonic recordings in vocalizing horseshoe bats that self-stimulation by the emitted pulse corresponds to an acoustic stimulus of ~ 78 – 83 dB SPL at the frequency of the second harmonic. Assuming that the acoustic transmission for the first and second harmonic is comparable, the ear will be stimulated by the emitted vocalization at the lower harmonic frequency at 40 – 70 dB SPL (i.e. 10 – 40 dB less than the second harmonic). This coincides well with the optimal intensity range of the lower frequency component in combination-sensitive neurons.

It is unclear what influence the relatively strong acoustic stimulation by the second harmonic in the emitted pulse has on the facilitated neurons. In the moustached bat, adding this frequency to the initial pulse often reduced the facilitation, thereby contracting and sharpening the delay–tuning curve boundaries (O'Neill and Suga, 1982).

Despite being the probable source of the lower frequency component

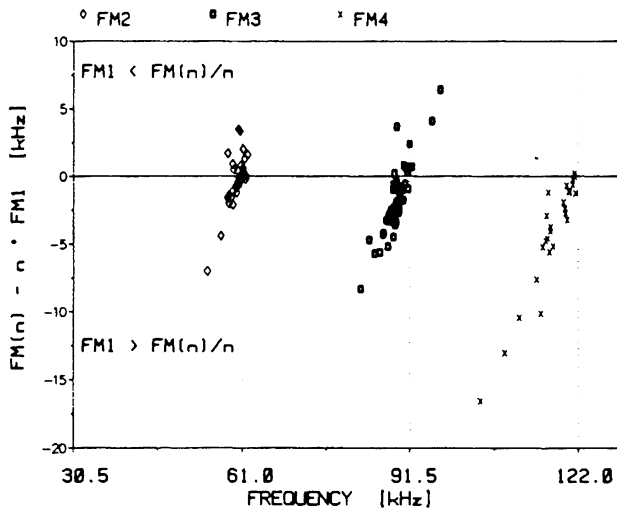


FIG. 17. Relation between best low-frequency and best high-frequency components for FM–FM facilitation represented as deviation from harmonic relationship ($F_n - n \times F_1$, $n = 2, 3, 4$, ordinate). Negative values mean that the low best frequency was higher or the high best frequency was lower than a harmonic relationship would require. The vertical dotted lines indicate the frequency of the different harmonics (normalized to a second harmonic of 61 kHz) as they occur in the orientation calls. The horizontal line at zero indicates harmonic frequency relationship of the components.

for facilitation, the vocalization can also have an adverse effect on facilitated neurons. On several occasions when vocalization occurred spontaneously during recording, the response of FM–FM neurons was shut down for several stimulus presentations (Fig. 9). However, in these cases, vocal self-stimulation was temporally uncorrelated with the stimulus ‘echoes’. What effect vocalization would have when the bat’s own vocalization is immediately followed by a corresponding echo is at present unknown for horseshoe bats. In moustached bats, Kawasaki et al. (1988) reported no difference in delay tuning or facilitation magnitude when FM–FM neurons were stimulated with pairs of artificial pulses and echoes versus artificial echoes time-locked to the bat’s own vocalizations. That ongoing vocalization alters processing of other types of acoustic signals in a time-dependent fashion has been shown in horseshoe bats (Schuller, 1979; Metzner, 1989). The shut-down of combination-sensitive cells by temporally uncorrelated vocalizations supports the evidence for a temporal analysis window for echoes tied to vocalization (Schuller, 1977; Roverud and Grinnell, 1985). It suggests that the processing of echoes falling outside the window might be actively suppressed by the bat’s vocalization, thus helping the bat avoid jamming by echolocating conspecifics.

Vocalizations in horseshoe bats can contain an initial upward frequency sweep at significant intensity levels. Strong initial frequency sweeps can have dramatic suppressive effects on the response properties of FM–FM neurons (Fig. 8). This affords the bat the possibility of controlling the activation of range-encoding cortical neurons by modulating the initial upward frequency sweep of the echolocation call.

Doppler-shift compensation and facilitated neurons

When a bat is hunting, the frequency of its emitted echolocation calls will be shifted upwards due to the Doppler shifts induced by its relative speed towards the target. The echo frequencies, consisting mainly of the second harmonic in the horseshoe bat and the second to fourth harmonics in the moustached bat, are thus higher than a harmonic interval

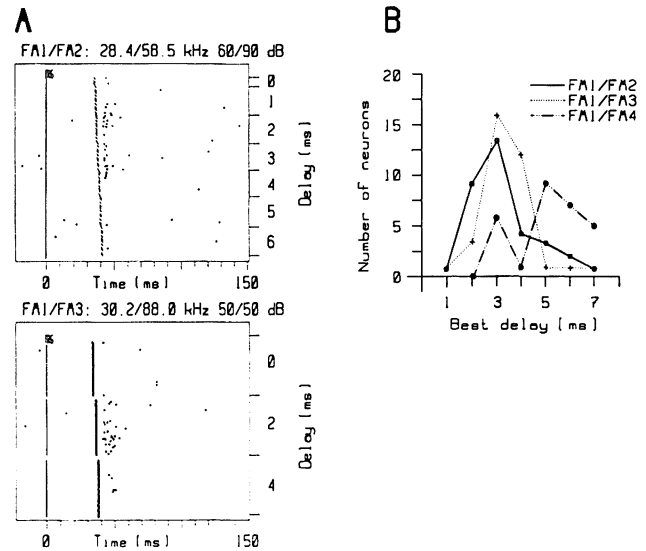


FIG. 18. Delay dependence of facilitated responses. The delay tuning is represented in the two graphs on the left, in which the temporal delay of the high-frequency component is changed stepwise between 1 and 6 ms (top) or 0 and 4 ms (bottom). The curves on the right give the distribution of best delays of FM–FM neurons for the three combinations FM1–FM2, FM1–FM3 and FM1–FM4. The distributions indicate an overrepresentation of facilitated neurons with best delays between 2 and 4 ms.

above the emitted fundamental. If the bat compensates for the induced Doppler shifts all frequencies are shifted in the same direction (lowered), but the non harmonic relationship will not be altered. The frequency tuning properties of facilitated neurons, however, show that best frequencies for facilitation in both species (Figs 4 and 17) show just the opposite trend. In the majority of neurons the upper harmonics are lower than a harmonic interval above the fundamental. Therefore it appears that the neurons are not optimally tuned to process composite signals as they occur during echolocation.

Yet, processing can occur within the frequency tuning range of the lower and upper component for facilitated response. The tuning of the upper component in most FM–FM neurons is close to the resting frequency, and is relatively sharp (bandwidth of only a few kHz), whereas the frequency tuning of the lower component is broad (5–15 kHz bandwidth). This means that normally the echo frequencies (FM component), whether shifted or not, will fall in the response area. Similarly, the lower harmonic of the echolocation call, either at rest or lowered during Doppler shift compensation, will fall within the tuning area for the lower facilitation component.

The consequence is that in real echolocation most FM–FM neurons will be facilitated suboptimally to some degree, but only a few will be stimulated by their optimal combination. The ‘frequency-tolerant’ behaviour (i.e. wide bandwidth) of the system avoids the situation where only a small proportion of the total population would be active for any particular pulse–echo frequency combination. The advantage of frequency-tolerant tuning properties for delay-sensitive neurons for delay evaluation has been discussed more fully elsewhere (O’Neill, 1985).

Best facilitation frequencies for CF/CF neurons

Although our sample of CF/CF facilitated neurons is small ($n = 23$ pure CF/CF and $n = 27$ mixed CFM–CFM), it is astonishing that only eight neurons had upper BFFs at or slightly above the resting frequency of

the bat. Most BFFs were in the range of the FM sweep frequencies. This finding differs from that in the moustached bat, where CF/CF neurons showed BFFs predominantly at or slightly above the corresponding harmonic (Suga *et al.*, 1983a,b).

In mixed CFM-type neurons that were facilitated by CF as well as FM combinations, the upper BFF generally fell within the FM2 sweep. The most probable explanation for this would be that facilitation of these neurons is not dependent on the particular temporal order of the facilitating frequencies presented. This view is supported by the fact that in many neurons the facilitation could also be produced with upward frequency sweeps or sinusoidal modulations, as long as the appropriate frequency range was involved. Often the order of frequency presentation had only a minimal effect on the level of response activity.

In the moustached bat, Suga *et al.* (1983b) showed that a bicoordinate map of upper and lower BFFs could be discerned in the area containing CF/CF cells. They postulated that CF/CF neurons encode the magnitude of the Doppler shift between the pulse and echo, and might function in the calculation needed for Doppler shift compensation. In the horseshoe bat, however, the tuning of CF/CF cells apparently does not correspond to the stimulus situation typical of Doppler compensation. CF/CF-facilitated neurons in horseshoe bats clearly require more extensive investigation before their significance in behaviour can be understood.

Temporal tuning of responses

Even more than frequency, the most important parameter for facilitation is the delay between the two components. Best delays are characteristic for facilitated neurons at the optimal frequencies and intensities of the two components. The facilitation shows a form of tuning to the delay, and the half-value of the response is typically reached at 1.5 ms for best delays between 2 and 4 ms (Fig. 6). If we take into account the fact that slight shifts of the best delay occur with changes in stimulus frequencies and/or intensities, individual cortical neurons can encode delay with only modest accuracy in the horseshoe bat. A typical neuron with a best delay of 3 ms, corresponding to a target distance of ~ 50 cm, would respond between 50 and 100% of maximum over distances between 26 and 76 cm. Ranges below 50 cm would not be distinguishable from those above on the basis of a discharge rate code alone. This means that, by itself, the firing rate of facilitated neurons is insufficient to provide unambiguous range information. FM–FM cells are not very precise range encoders. But the cortical system employs many such cells, and it must somehow provide a reasonable approximation of the accuracy that these bats achieve in behavioural experiments on range discrimination (Simmons, 1971, 1973). Reversible inactivation (with the GABA agonist muscimol) in the FM–FM area in moustached bats selectively disrupts fine time delay discrimination of FM–FM stimulus pairs (Riquimaroux *et al.*, 1991), suggesting the importance of cortical processing to this perception. Parallel processing of range information by many neurons might be a reasonable explanation for the behaviourally measured performance. The power of cortical maps in providing vector sums of the actual value of a stimulus parameter to yield extremely high acuity is discussed in Altes (1989).

Topographical arrangement of best delays

In the dorsal part of the horseshoe bat auditory cortex, we did not find multiple representations of best delay gradients as reported in the moustached bat (Suga and Horikawa, 1986). Only one field showed a rostrocaudal gradient of increasing best delay. Delays of <2 ms or >5 ms were rarely found, in agreement with the findings in the

moustached bat (O'Neill and Suga, 1982). The numerical overrepresentation of best delays between 2 and 4 ms (Fig. 5) was reflected in the topographical distribution (Fig. 12). In contrast to the findings in the moustached bat (Suga and Horikawa, 1986), the rostrocaudal change in best delay is not linear. Rather, there is an enlargement of the cortical space devoted to best delays ~ 3 ms (~ 50 cm). Seventy per cent of the rostrocaudal distance occupied by FM–FM neurons is devoted to best delays <4 ms, and 64% of this area represents best delays between 2 and 4 ms. In earlier reports (O'Neill and Suga, 1982; Suga *et al.*, 1983b) a numerical and spatial overrepresentation of best delays between 3 and 8 ms (maximum at 4–6 ms) is reported for the FM–FM area of the moustached bat.

Supplementary functional interpretation for facilitated neurons

The overrepresentation of best delays ~ 3 ms suggests an alternative to the notion that the FM–FM region simply forms a map of target distance. Perhaps the activation of neurons in this area acts to trigger the behaviours used to intercept a volant target. The following scenario illustrates this idea. When the bat is at some distance from the target, only a few FM–FM neurons would be activated. Subsequently, as the bat approaches the prey, the activation would progress from caudal to more rostral sites. Not only would the position of peak activity move in the dorsal field, but also the number of neurons activated would increase very abruptly as the bat flew to within 76 cm of the target, reaching a maximum at ~ 50 cm, corresponding to a delay of ~ 3 ms. The sharp increase and maximization of activity at these distances might trigger the motor responses needed to capture the prey.

When considering this alternative hypothesis, it is important to keep in mind that any flight manoeuvre necessitates a minimal time to be initiated prior to the encounter, and that this time depends on the flight speed and the radius of the turn (Norberg *et al.*, 1987). Thus an insect can escape if it manages to perform quicker turns than the bat, due to the vastly different inertial masses (a good example of this can be found in Trappe and Schnitzler, 1982). A bat flying at speeds of 2–4 m/s can cover a distance of 50 cm in a time span of 250–125 ms. It is unlikely that it has much freedom to control its flight path within the last 100–200 ms of target pursuit: the bat becomes essentially ballistic in the final approach. The same logic suggests that the final manoeuvres before capture must be made some 200 ms in advance.

Since the bat often catches an insect using its wings and its interfemoral membrane (uropatagium), it will have a good chance of success if the posture assumed at a distance between 76 and 50 cm from the target is simply maintained for the rest of the capture sequence. The high level of activity arising in delay-tuned dorsal cortical neurons at these distances might therefore be the signal to make body position adjustments for prey capture, which then follows in a rather independent way. The same mechanism could be involved in obstacle crash avoidance or in landing manoeuvres, by triggering the appropriate turns at the right time.

This 'alarm' hypothesis is not meant to exclude the common functional interpretation that these neurons precisely measure target distance and translate it to topographical coordinates in a cortical map. Rather, it tries to present an explanation for the strong overrepresentation of distinct temporal delays ~ 3 ms and the non-linearity of the delay mapping on the cortical axis.

Acknowledgements

We are indebted to G. Franke and E. Biberger for technical help. Supported by Deutsche Forschungsgemeinschaft, Sonderforschungsbereich 204 (Gehör), Teilprojekt 10 and Z.

Abbreviations

BFF	best facilitation frequency
CF	constant frequency
CN _n	component <i>n</i> of CF stimulus
CFM	CF followed by FM stimulus
FM	frequency modulation
FM _n	component <i>n</i> of FM stimulus
GABA	γ-aminobutyric acid
SFM	sinusoidally frequency-modulated

References

- Altes, R. A. (1989) Ubiquity of hyperacuity. *J. Acoust. Soc. Am.*, **85**, 943–952.
- Asanuma, A., Wong, D. and Suga, N. (1983) Frequency and amplitude representations in anterior primary auditory cortex of the mustached bat. *J. Neurophysiol.*, **50**, 1182–1196.
- Belwood, J. and Morris, G. K. (1987) Bat predation and its influence on calling behavior in neotropical katydids. *Science*, **238**, 64–67.
- Berkowitz, A., Suga, N. (1989) Neural mechanisms of ranging are different in two species of bats. *Hear. Res.*, **B41B**, 255–264.
- Brugge, J. F. and Merzenich, M. M. (1973) Responses of neurons in auditory cortex of the macaque monkey to monaural and binaural stimulation. *J. Neurophysiol.*, **36**, 1138–1158.
- Kawasaki, M., Margoliash, D. and Suga, N. (1988) Delay-tuned combination-sensitive neurons in the auditory cortex of the vocalizing mustached bat. *J. Neurophysiol.*, **B59B**, 623–635.
- Link, A., Marimuthu, G. and Neuweiler, G. (1986) Movement as a specific stimulus for prey catching behaviour in rhinolophoid and hipposiderid bats. *J. Comp. Physiol. A*, **159**, 403–413.
- Merzenich, M. M., Knight, P., Roth, G. L. (1975) Representation of cochlea within primary auditory cortex in the cat. *J. Neurol.*, **38**, 231–249.
- Metzner, W. (1989) A possible neuronal basis for Doppler-shift compensation in echo locating horseshoe bats. *Nature*, **B341B**, 529–532.
- Neuweiler, G., Metzner, W., Ruebsamen, R., Eckrich, M. and Costa, H. H. (1987) Foraging behavior and echolocation in the rufous horseshoe bat *Rhinolophus rouxi* of Sri Lanka. *Behav. Ecol. Sociobiol.*, **20**, 53–57.
- Norberg, U. M. and Rayner, J. M. V. (1987) Ecological morphology and flights in bats (Mammalia: Chiroptera): wing adaptation, flight performance, foraging strategy and echolocation. *Phil. Trans. R. Soc. London, Ser. B*, **316**, 337–419.
- O'Neill, W. E. (1985) Responses to pure tones and linear FM components of the CF–FM biosonar signal by single units in the inferior colliculus of the mustached bat. *J. Comp. Physiol. A*, **157**, 797–815.
- O'Neill, W. E. and Suga, N. (1979) Target range-sensitive neurons in the auditory cortex of the mustached bat. *Science*, **203**, 69–73.
- O'Neill, W. E. and Suga, N. (1982) Encoding of target-range and its representation in the auditory cortex of the mustached bat. *J. Neurosci.*, **2**, 17–31.
- Ostwald, J. (1980) Die funktionelle Organisation des Hörcortex der grossen Hufeisennase, *Rhinolophus ferrumequinum*. Inaugural Dissertation, University of Frankfurt, FRG.
- Ostwald, J. (1984) Tonotopical organization and pure tone response characteristics of single units in the auditory cortex of the greater horseshoe bat. *J. Comp. Physiol. A*, **155**, 821–834.
- Pietsch, G. and Schuller, G. (1987) Auditory self-stimulation by vocalization in the CF–FM bat, *Rhinolophus rouxi*. *J. Comp. Physiol. A*, **160**, 635–644.
- Reale, R. A. and Imig, T. J. (1980) Tonotopic organization in auditory cortex of the cat. *J. Comp. Neurol.*, **192**, 265–291.
- Riquimaroux, H., Gaioni, S. J. and Suga, N. (1991) Cortical computational maps control auditory perception. *Science*, **251**, 565–568.
- Roverud, R. G. and Grinnell, A. D. (1985) Echolocation sound features processed to provide distance information in the CF/FM bat, *Noctilio albiventris*: evidence for a gated time window utilizing both CF and FM components. *J. Comp. Physiol. A*, **156**, 457–469.
- Schnitzler, H. U. (1968) Die Ultraschall-Ortungslaute der Hufeisen-Fledermaeuse (Chiroptera-Rhinolophidae) in verschiedenen Orientierungssituationen. *Z. Vergl. Physiol.*, **57**, 376–408.
- Schnitzler, H. U. (1970) Echoortung bei der Fledermaus *Chilonycteris rubiginosa*. *Z. Vergl. Physiol.*, **68**, 25–38.
- Schreiner, C. E. and Urbas, J. V. (1988) Representation of amplitude modulation in the auditory cortex of the cat. II. Comparison between cortical fields. *Hear. Res.*, **32**, 49–64.
- Schuller, G. (1977) Echo delay and overlap with emitted orientation sounds and Doppler compensation in the bat, *Rhinolophus ferrumequinum*. *J. Comp. Physiol.*, **114**, 103–114.
- Schuller, G. (1979) Vocalization influences auditory processing in collicular neurons of the CF–FM bat, *Rhinolophus ferrumequinum*. *J. Comp. Physiol.*, **132**, 39–46.
- Schuller, G., Beuter, K. and Schnitzler, H. U. (1974) Response to frequency shifted artificial echoes in the bat *Rhinolophus ferrumequinum*. *J. Comp. Physiol.*, **89**, 275–286.
- Schuller, G., Radtke-Schuller, S. and Betz, M. (1986) A stereotaxic method for small animals using experimentally determined reference profiles. *J. Neurosci. Methods*, **18**, 339–350.
- Schuller, G., Radtke-Schuller, S. and O'Neill, W. E. (1988) Processing of paired biosonar signals in the cortices of *Rhinolophus rouxi* and *Pteronotus p. parnellii*: a comparative neurophysiological and neuroanatomical study. In Nachtigall, P. E. and Moore, P. W. B. (eds), *Animal Sonar Processes and Performance*. Plenum Press, New York and London, pp. 259–264.
- Schweizer, H. and Radtke, S. (1980) The auditory pathway of the greater horseshoe bat, *Rhinolophus ferrumequinum*. In Busnel, R.-G. and Fish, J. F. (eds), *Animal Sonar Systems*. Plenum Press, New York and London, pp. 987–989.
- Simmons, J. A. (1971) The sonar receiver of the bat. *Ann. N. Y. Acad. Sci.*, **188**, 161–174.
- Simmons, J. A. (1973) The resolution of target range by echolocating bats. *J. Acoust. Soc. Am.*, **54**, 157–173.
- Suga, N. (1978) Specialization of the auditory system for reception and processing species-specific sounds. *Fed. Proc.*, **37**, 2342–2354.
- Suga, N. (1984) Neural mechanisms of complex-sound processing for echolocation. *Trends Neurosci.*, **1**, 20–27.
- Suga, N. and Horikawa, J. (1986) Multiple time axis for representation of echo delays in the auditory cortex of the mustached bat. *J. Neurophysiol.*, **55**, 776–805.
- Suga, N., and Jen, P.-S. (1976) Disproportionate tonotopic representation for processing CF–FM sonar signals in the mustached bat auditory cortex. *Science*, **194**, 542–544.
- Suga, N. and Manabe, T. (1982) Neural basis of amplitude-spectrum representation in auditory cortex of the mustached bat. *J. Neurophysiol.*, **47**, 225–255.
- Suga, N. and O'Neill, W. E. (1979) Neural axis representing target range in the auditory cortex of the mustached bat. *Science*, **206**, 351–353.
- Suga, N., O'Neill, W. E. and Manabe, T. (1978) Cortical neurons sensitive to combinations of information-bearing biosonar signals in the mustached bat. *Science*, **200**, 778–781.
- Suga, N., O'Neill, W. E. and Manabe, T. (1979) Harmonic-sensitive neurons in the auditory cortex of the mustached bat. *Science*, **203**, 270–273.
- Suga, N., Niwa, H. and Taniguchi, I. (1983a) Representation of biosonar information in the auditory cortex of the mustached bat, with emphasis on representation of target velocity information. In Ewert, J. P., Capranica, R. R. and Ingle, D. J. (eds), *Advances in Vertebrate Neuroethology*. Plenum Press, New York and London, pp. 829–867.
- Suga, N., O'Neill, W. E., Kujirai, K. and Manabe, T. (1983b) Specificity of combination-sensitive neurons for processing of complex biosonar signals in auditory cortex of the mustached bat. *J. Neurophysiol.*, **49**, 1573–1626.
- Sullivan, W. E. (1982a) Neural representation of target distance in auditory cortex of the echolocating bat *Myotis lucifugus*. *J. Neurophysiol.*, **48**, 1011–1032.
- Sullivan, W. E. (1982b) Possible neural mechanisms of target distance coding in auditory system of the echolocating bat *Myotis lucifugus*. *J. Neurophysiol.*, **48**, 1033–1047.
- Trappe, M. and Schnitzler, H. U. (1982) Doppler-shift compensation in insect-catching horseshoe bats. *Naturwissenschaften*, **69**, 193–194.
- Wong, D. and Shannon, S. L. (1988) Functional zones in the auditory cortex of the echolocating bat, *Myotis lucifugus*. *Brain Res.*, **453**, 349–352.
- Woolsey, C. N. and Walzl, E. M. (1941) Topical projection of nerve fibers from local regions of the cochlea to the cerebral cortex of the cat. *Am. J. Physiol.*, **133**, 498–499.

The European Journal of Neuroscience

Forthcoming papers include:

RESEARCH PAPERS

Pharmacological and Electrophysiological Properties of Recombinant GABA_A Receptors Comprising the $\alpha 3$, $\beta 1$ and $\gamma 2$ Subunits

F. Knoflach, K. H. Backus, T. Giller, P. Malherbe, P. Pflimlin, H. Möhler and G. Trube

Long-term Depression of Glutamate Currents in Cultured Cerebellar Purkinje Neurons Does Not Require Nitric Oxide Signalling

D. J. Linden and J. A. Connor

Synaptic Activation of GABA_A Receptors Causes a Depolarizing Potential Under Physiological Conditions in Rat Hippocampal Pyramidal Cells

M. Avoli

The Critical Period for Experience-dependent Plasticity in a System of Binocular Visual Connections in *Xenopus laevis*: Its Temporal Profile and Relation to Normal Developmental Requirements

M. J. Keating and S. Grant

The Critical Period for Experience-dependent Plasticity in a System of Binocular Visual Connections in *Xenopus laevis*: Its Extension by Dark-rearing

S. Grant, E. A. Dawes and M. J. Keating

High Resolution Light and Electron Microscopic Immunocytochemistry of Co-localized GABA and Calbindin D-28k in Somata and Double Bouquet Cell Axons of Monkey Somatosensory Cortex

J. DeFelipe and E. G. Jones

Calbindin-D28K (CaBP_{28K})-like Immunoreactivity in Ascending Projections I. Trigeminal Nucleus Caudalis and Dorsal Vagal Complex Projections

D. Menétrey, J. de Pommery, K. G. Baimbridge and M. Thomasset

Calbindin-D28K (CaBP_{28K})-like Immunoreactivity in Ascending Projections II. Spinal Projections to Brain Stem and Mesencephalic Areas

D. Menétrey, J. de Pommery, M. Thomasset and K. G. Baimbridge

Heterotopic Cortical Afferents to the Medial Prefrontal Cortex in the Rat. A Combined Retrograde and Anterograde Tracer Study

C. G. Van Eden, V. A. F. Lamme and H. B. M. Uylings

Contrasting Effects of Raclopride and SCH 23390 on the Cellular Content of Preproenkephalin A mRNA in Rat Striatum: A Quantitative Non Radioactive *In Situ* Hybridization Study

S. J. Augood, R. L. M. Faull and P. C. Emson

SHORT COMMUNICATIONS

Two GTP-binding Proteins Control Calcium-dependent Exocytosis in Chromaffin Cells

J.-M. Sontag, D. Aunis and M.-F. Bader

Putative Single Quantum and Single Fibre Excitatory Postsynaptic Currents Show Similar Amplitude Range and Variability in Rat Hippocampal Slices

M. Raastad, J. F. Storm and P. Andersen

Author index

- Aguiayo, A.J. 758
Aicardi, G. 866
Albowitz, B. 570
Alford, S. 107
Alvarez, J. 1123
Álvarez-Bolado, G. 118
Amitai, Y. 47
Andersson, T. 66
Anokhin, K.V. 162
Arvidsson, U. 737
Ashley, C.C. 349
- Bacon, S.J. 55
Bahro, M. 366
Barakat-Walter, I. 431
Barker, J.L. 72
Battaglini, P.P. 452
Batten, T.F.C. 501
Bédard, S. 1016
Ben Ari, Y. 301, 523, 962
Benham, C.D. 285
Bennett-Clarke, C.A. 1255
Bensouilah, M. 407
Bentivoglio, M. 118, 1008
Berretta, N. 850
Berton, F. 850
Besse, D. 1343
Besson, J.M. 1343
Bianchi, R. 850
Bigot, D. 551
Bijak, M. 473
Bilbaut, A. 10
Björklund, A. 86, 905
Blanc, G. 1001
Bockaert, J. 778, 928, 1338
Boer, G.J. 154
Bohm, C. 481
Bosler, O. 1330
Bossu, J.L. 771, 778
Boulton, C.L. 992
Bourne, R.C. 243
Boutelle, M.G. 940
Bouvier, M.M. 285
Boycott, B.B. 1069
Brady, M.J. 441
Bramham, C.R. 1300
Braschler, U.F. 1037
Brener, K. 47
Brenneman, D.E. 32
Brown, D.A. 820
Brown, M.C. 102, 1366
Brun, P. 397
Brunelli, M. 850
Buckmaster, A. 698
Buda, M. 397
Bueno-López, J.L. 415
Buisson, B. 928
Bullier, J. 186
Buonviso, N. 493
Burke, W. 1245
Burls, A. 216
Bustos, J. 1123
Buzsáki, G. 222
- Cadelli, D. 825
Caliebe, F. 18
Cameron-Curry, P. 126
- Canlon, B. 1338
Capogna, M. 850
Caretta, A. 669
Carmody, J. 833
Carter, D.A. 758
Casseday, J.H. 648
Cattaert, D. 1219
Caulfield, M.P. 820
Cenci, M.A. 905
Cevolani, D. 669
Chamak, B. 1155
Cherubini, E. 301, 523, 962
Christenson, J. 107
Clarac, F. 1208, 1219
Cobo, M. 531
Condé, F. 855
Conley, M. 237, 1089
Cooper, M. 243
Cordier, J. 539
Corner, M.A. 140
Corradetti, R. 301
Corsini, G.U. 72
Côté, P.-Y. 1316
Cottee, L.J. 1245
Covey, E. 648
Cowey, A. 802
Crépel, F. 855
Csillag, A. 243
Cuénod, M. 201, 366, 1370
Cullheim, S. 737
Curtis, R. 876
- Dagerlind, Å. 737
Dale, N. 1025
Daszuta, A. 1330
Davies, D.C. 243
de Pommery, J. 249
de Barry, J. 1146
De Waard, M. 771
Dean, P. 790
Delumeau, J.C. 539
Denizot, J.-P. 407
di Porzio, U. 72
Di Stefano, M. 1016
Diamond, I.T. 237, 1089
DiCaprio, R.A. 1219
Do, K.Q. 201, 1370
Dulac, C. 126
Dumoulin, F.L. 338
Dumuis, A. 928
Durand, J. 621
Dutar, P. 839
- Eagles, D.A. 441
Eaton, S.A. 296, 1104
Eder, C. 1271
Edwards, S.N. 698
Eiden, L.E. 32
El Manira, A. 1208, 1219
Emson, P.C. 839
Ernfors, P. 953
Evan, G. 887
Evans, M.L. 285
Eysel, U.T. 1232
- Fagni, L. 778
Fahrig, T. 634
- Fairén, A. 118
Fattori, P. 452
Faúndez, V. 1123
Féger, J. 947
Feltz, A. 771
Ficker, E. 1271
Figley, B. 1255
Fillenz, M. 940
Fischer-Colbrie, R. 895
Fish, S.E. 1255
Fitzgerald, M. 383
FitzGibbon, T. 1245
Forloni, G.L. 40
Foster, G.A. 32
Francesconi, W. 850
Friedman, W.J. 688
Fusco, M. 1008
- Gaffan, D. 615
Gähwiler, B.H. 343
Gaiarsa, J.-L. 301
Galletti, C. 452
Gallimore, P.H. 663
Garthwaite, G. 715, 729
Garthwaite, J. 379, 715, 729
Gehrmann, J. 919
Giuffrida, R. 866
Glickstein, M. 317
Glowinski, J. 539, 1001
Gombos, G. 764
Gómez-Urquijo, S.M. 415
Gondra, J. 415
Gonon, F. 397
Grabham, P.W. 663
Graeber, M.B. 919
Grand, R.J.A. 663
Grandes, P. 415, 1370
Greenfield, S.A. 292
Greitz, T. 481
Grillner, S. 107
Grubb, B.D. 981
Grunditz, T. 331
Guidolin, D. 1008
Guillemot, J.P. 1016
Gündel, J. 1271
Gundersen, V. 1281
Gutnick, M.J. 47
- Haas, C.A. 708
Hamon, B. 855
Hardy, R. 876
Häußler, J. 18
Heinemann, U. 1271
Hennequet, L. 415
Henry, G.H. 186
Hernandez-Nicaise, M.L. 10
Heywood, C.A. 802
Higashida, H. 820
Hoffmann, P. 18
Hökfelt, T. 737
Homburger, V. 1338
Hunt, S.P. 551, 887
- Ibáñez, C.F. 1309
Illert, M. 18
Innocenti, G.M. 1134
Ito, S. 962
- Jaillard, D. 855
Jean, A. 1353
Jefferys, J.G.R. 47
Jockusch, H. 1182
Johnson, H. 737
Jones, S.A. 292
Jourdan, F. 493
Julien, J.-P. 758
- Kalén, P. 905
Katz, L.C. 1
Kaupmann, K. 1182
Keicher, E. 10
Kennedy, B. 222
Kettenmann, H. 230, 310, 813
Kilpatrick, I.C. 971
King, S.M. 790
Kittel, P.W. 209
Kivipelto, L. 175
Klinz, S. 634
Knodler, L. 833
Knöpfel, T. 343
Kopin, I.J. 72
Kreutzberg, G.W. 338, 708, 919
Kristensson, K. 66
Kudo, Y. 1146
Kuhnt, U. 570
Kupersmith, A.C. 1089
- Lachuer, J. 397
Lagenaur, C.F. 86
Lamour, Y. 839
Le Douarin, N.M. 126
Legg, C.R. 317
Leon, A. 1008
Lepore, F. 1016
Lewin, G.R. 1112
Lindstrand, K. 331
Lindvall, O. 905
Lombard, M.C. 1343
López, R. 559
López-Medina, A. 415
Löve, A. 66
Lowrie, M.B. 216
Luiten, P.G.M. 168
Lund, R.D. 86
Lunn, E.R. 102, 1366
Luppino, G. 669
Lüscher, H.-R. 1037, 1054
Luts, A. 331
Lynn, B. 274
- Mackay-Sim, A. 209
Maggio, K. 10
Mahata, M. 895
Mahata, S.K. 895
Mallat, M. 1155
Maqbool, A. 501
Marin, P. 539
Markel, É. 168
Marksteiner, J. 895
Marocco, C. 1330
Marrero, H. 813
Marzi, C.A. 1016
Masetto, S. 514
Matelli, M. 669
Matus, A. 551

Author index

- McMahon, S.B. 1112
 McWilliam, P.N. 501
 Menétrey, D. 249
 Milgram, N.W. 1300
 Misgeld, U. 473
 Moffett, J.R. 441
 Monard, D. 663
 Montavon, P. 331
 Mooney, R.D. 1255
 Mora, F. 531
 Morino, P. 366, 1370
 Müller, W. 473
 Murray, S. 833
- Nambodiri, M.A.A. 441
 Neal, J.W. 971
 Neale, J.H. 441
 Neugebauer, V. 981
 Neuman, R. 523
 Newcombe, F. 802
 Nicaise, G. 10
 Nobes, C.D. 698
 Nyakas, C. 168
- O'Neill, W.E. 1165
 O'Shaughnessy, C.T. 992
 Ogura, A. 1146
 Olson, L. 688
 Oomagari, K. 928
 Oppmann, M. 981
 Orkand, P.M. 813
 Orkand, R.K. 813
 Ottersen, O.P. 1281
- Panula, P. 175
 Parent, A. 1316
 Pearson, R.C.A. 971
 Pérez-Méndez, L. 559
 Perry, V.H. 102, 1366
 Persson, H. 688, 953, 1309
 Pesheva, P. 356
 Peterson, A. 758
 Piehl, F. 737
 Pin, J.-P. 928
 Pini, A. 274
 Polato, P. 1008
 Potier, B. 839
 Powell, T.P.S. 971
 Prada, C. 559
 Prémont, J. 539
 Probstmeier, R. 356
 Provini, L. 962
 Püto, M. 1016
 Puga, J. 559
- Raadsheer, F.C. 140
 Radpour, S. 587, 602
 Radtke-Schuller, S. 1165
 Raivich, G. 338, 919
 Ramaekers, F.C.S. 140
 Ramakers, G.J.A. 140, 155
 Ramirez, G. 559
 Rapisarda, C. 866
 Reblet, C. 415
 Reddington, M. 708
 Redgrave, P. 790
 Revial, M.F. 493
 Reynolds, R. 876
 Rhoades, R.W. 1255
 Riederer, B.M. 431, 1134
 Rizzi, M. 40
 Robbins, J. 820
- Robledo, P. 947
 Roland, P.E. 481
 Rose, S.P.R. 162
 Rossi, P. 514
- Sadikot, A.F. 1316
 Sakurai-Yamashita, Y. 764
 Sala, S. 462
 Salin, P.A. 186
 Salt, T.E. 296, 1104
 Samanin, R. 40
 Sánchez, M.P. 118
 Sassone-Corsi, P. 764
 Schachner, M. 230, 356, 634
 Schaible, H.-G. 981
 Schirrmacher, J. 18
 Schmechel, D.E. 237
 Schuller, G. 648, 1165
 Schultzberg, M. 66
 Schuurman, T. 168
 Schwab, M.E. 825
 Schwarcz, R. 66
 Seitz, R.J. 481
 Sendtner, M. 1182
 Senut, M.C. 839
 Serafini, R. 40
 Shortland, P. 383
 Simon, H. 634
 Smith, A.D. 260
 Solt, V.B. 222
 Sontheimer, H. 230
 Soria, B. 462
 Southam, E. 379
 Spenger, C. 1037, 1054
 Sperk, G. 895
 Spiess, E. 356
 Spreafico, R. 118
 Spruce, B.A. 876
 Srebro, B. 1300
 Staub, C. 343
 Stewart, M.G. 243
 Stöckli, K.A. 1182
 Stone-Elander, S. 481
 Storm-Mathisen, J. 1281
 Streit, J. 1037, 1054
 Streit, P. 366, 1370
 Streit, W.J. 338
 Suaud-Chagny, M.F. 397
 Subramaniam Krishnan 216
 Sundler, F. 331
 Supattapone, S. 349
- Taglietti, V. 514
 Tassin, J.-P. 1001
 Tell, F. 1353
 Tencé, M. 539
 Terenius, L. 737
 Thanos, S. 1189
 Théry, C. 1155
 Thomasset, M. 855
 Thomson, A.M. 587, 602
 Tirindelli, R. 669
 Tolkovsky, A.M. 698
 Toselli, M. 514
 Trotter, J. 230, 310
- Uddman, R. 331
 Ulfhake, B. 737
- van Leeuwen, F.W. 140
 Vantini, G. 1008
 Vaudano, E. 317
- Vezina, P. 1001
 Vezzani, A. 40
 Vial, J.D. 1123
 Vidal-Sanz, M. 758
 Villar, M. 737
 Villegas-Pérez, M.P. 758
 Vollenweider, F.X. 201
 von Blankenfeld, G. 310
 Von Krosigk, M. 260
 Vranesic, I. 343
 Vrbová, G. 216
- Wässle, H. 1069
 Watkins, S. 615
 Westland, K. 1245
 Wheeler, D.B. 940
 Wickman, C. 66
 Victorin, K. 86
 Wiedemann, E. 18
 Wilkin, G.P. 876
 Williams, S. 887
 Williamson, L.C. 441
 Winkler, H. 895
 Wörgötter, F. 1232
 Wouterlood, F.G. 641
- Zagon, A. 55
 Zetterström, T. 940
 Ziegler, M. 222
 Zollinger, M. 201
 Zuddas, A. 72

Subject index

Abducens

motor neurons, intracellular recording, *N*-methyl-D-aspartate, rat 621

Acetylcholine

receptors, muscarinic, neuroblastoma, transfected cells, M-current 820

Acetylcholinesterase

release, substantia nigra, locomotion, light-emitting reaction, guinea-pig 292

Achromatopsia

cerebral, hue discrimination, man 802

Adenosine

release, cerebellum, climbing fibres, deprivation, rat 201

Adrenoreceptors

astrocytes, calcium, mouse 539

thalamus, oscillation, noradrenalin, rat 222

Age

calbindin, hippocampus, rat 839

nerve growth factor, neurons, reticular thalamic nucleus, rat 1008

α -amino-3-hydroxy-5-methyl-4-isoxazolepropionate

neurons, toxicity, brain, rat 715

neurons, toxicity, brain, rat 729

Amphetamine

D-1 dopamine receptors, medial prefrontal cortex, locomotion, rat 1001

Antigenic determinants

glia, Schwann cells, Japanese quail 126

Arachidonic acid

metabolites, release, glutamate, ionomycin, mouse 928

Ascorbate

release, striatum, dopamine, receptors, rat 940

Aspartate

hippocampus, depolarization, rat 1281

Asphyxia

behaviour, learning, open field, calcium, antagonists, rat 168

Astrocytes

arachidonic acid, metabolites, release, mouse 928

cerebellum, calcium, mobilization, *trans*-1-amino-

cyclopentyl-1,3-dicarboxylic acid, rat 1146

differentiation, growth-associated proteins, rat 876

Fos, induction, calcitonin gene-related peptides, rat 708

potassium channels, endothelins, rat 349

potassium channels, optic nerve, frog 813

ATP

receptors, sensory neurons, calcium, homeostasis, rat 285

Auditory cortex

cerebellum, connections, pontine grey, horseshoe bat 648

neurons, responses, complex sounds, bat 1165

projections, thalamic reticular nucleus, bushbabies 1089

Auditory system

guanine nucleotide binding proteins, guinea-pig 1338

Axons

growth, neuroepithelium, serine proteases, man 663

Barbiturates

nociception, GABA, receptors, mouse 833

Behaviour

open field, anoxia, calcium, antagonists, rat 168

Bioelectric activity

cerebral cortex, tetrodotoxin, *in vitro* culture, rat 154

Brain

basal nuclei, calcium-binding proteins, distribution, squirrel monkey 1316

brain-derived neurotrophic factor, expression, ontogeny, rat 688

chromogranins, messenger RNA, rat 895

corticorubral projections, guinea-pig 866

cyclic AMP, binding sites, synapses, rat 669

Fos, convulsants, mouse 764

macrophages, cytotoxicity, neurons, rat 1155

morphine-modulating peptides, enkephalin, rat 175

Brain spectrins

dorsal root ganglia, development, fowl 431

Brain stem

motor neurons, intracellular recording, *N*-methyl-D-aspartate, rat 621

swallowing area, rhythmic discharges, *N*-methyl-D-aspartate, rat 1353

Brain-derived neurotrophic factor

expression, brain, ontogeny, rat 688

messenger RNA, dorsal root ganglia, embryos, rat 953

C-fibres

regeneration, capsaicin, rat 274

Calbindin

distribution, basal nuclei, squirrel monkey 1316

hippocampus, calcium, homeostasis, age, rat 839

neurons, cerebellum, embryos, rat 855

Calcitonin gene-related peptide

facial motor nucleus, neurons, regeneration, rat 338

Fos, induction, astrocytes, rat 708

messenger RNA, motor neurons, spinal cord, lesions, rat 737

Calcium

astrocytes, striatum, adenosine, adrenoreceptors, arachidonic acid, mouse 539

calcium-binding proteins, distribution, basal nuclei, squirrel monkey 1316

calcium channels, antagonists, epileptiform activity, neocortex, rat 992

calcium currents, cerebellum, granule cells, rat 771

calcium currents, neuroblastoma, cell lines, man 514

currents, giant neurons, *Aplysia* 10

homeostasis, calbindin, hippocampus, age, rat 839

homeostasis, sensory neurons, ATP receptors, rat 285

mobilization, cerebellum, astrocytes, *trans*-1-amino-

cyclopentyl-1,3-dicarboxylic acid, rat 1146

Capsaicin

nociceptors, C-fibres, skin, rat 274

Catecholamines

locus coeruleus, sciatic nerve, stimulation, rat 397

Caudate-putamen

lesions, GABA, superior colliculus, rat 971

Cell lines

neuroblastoma, neural adhesion molecules, cross-linking, mouse 634

Cerebellum

adenosine, release, climbing fibres, deprivation, rat 201

astrocytes, calcium, mobilization, *trans*-1-amino-

cyclopentyl-1,3-dicarboxylic acid, rat 1146

auditory cortex, connections, pontine grey, horseshoe bat 648

climbing fibres, nitric oxide, rat 379

granule cells, calcium currents, rat 771

granule cells, potassium channels, activation, mouse 778

homocysteate, glia, rat 1370

neurons, toxicity, α -amino-3-hydroxy-5-methyl-4-isoxazolepropionate, rat 715

neurons, toxicity, α -amino-3-hydroxy-5-methyl-4-isoxazolepropionate, rat 729

Purkinje cells, climbing fibre responses, calcium, rat 343

Purkinje cells, embryos, rat 855

Cerebral cortex

bioelectric activity, cell death, *in vitro* culture, rat 154

bioelectric activity, *in vitro* culture, rat 140

D-1 dopamine receptors, locomotion, rat 1001

inverted cells, projection neurons, retrograde labelling, rabbit 415

lesions, GABA, superior colliculus, rat 971

projections, nucleus ruber, guinea-pig 866

Cerebrum

glycoproteins, long-term memory, chicken 243

mapping, somatosensory discrimination, man 481

Subject index

Choline acetyltransferase

gene expression, cell transfection, rat 1309

Chromaffin cells

potassium currents, inactivation, cattle 462

Chromogranins

messenger RNA, brain, rat 895

Circumvallate papilla

neurons, retrograde tracing, rat 331

Climbing fibres

cerebellum, nitric oxide, rat 379

climbing fibre responses, Purkinje cells, calcium, rat 343

deprivation, adenosine, release, cerebellum, rat 201

Colour

coding, retina, bipolar cells, morphological classification, rhesus monkey 1069

colour blindness, discrimination, man 802

Convulsants

Fos, brain, mouse 764

Corpus callosum

tau proteins, distribution, cat 1134

visual projections, enucleation, hamster 1255

Cutaneous sense organs

taste buds, *Astryanax jordani* 407

Cyclic AMP

binding sites, synapses, brain, rat 669

Cytoskeleton

corpus callosum, visual cortex, cat 1134

neurons, excitatory amino acids, rat 551

sural nerves, RNA, synthesis, inhibitors, rat 1123

DNA

nucleotide sequences, choline acetyltransferase, rat 1309

Dopamine

D-1 dopamine receptors, cerebral cortex, locomotion, rat 1001

receptors, ascorbate, release, striatum rat 940

Dorsal horn

opioid receptors, dorsal root C7, rat 1343

saphenous nerve, connections, sciatic nerve, section 383

sensory neurons, peripheral nerves, regeneration, rat 1112

Dorsal motor vagal nucleus

neurons, GABA, cat 501

Dorsal root

spinal cord, slice cultures, cytology, rat 1037

Dorsal root ganglia

brain-derived neurotrophic factor, messenger RNA, embryos, rat 953

neurons, regeneration, calcitonin gene-related peptide, rat 338

Echolocation

pontine grey, neurons, tuning, horseshoe bat 648

Embryos

locomotion, spinal cord, neurons, isolation, *Xenopus* 1025

Purkinje cells, *in vitro* development, rat 855

spinal cord, dorsal root, slice cultures, cytology, rat 1037

spinal cord, dorsal root, slice cultures, reflex arc, rat 1054

Endothelins

potassium channels, astrocytes, rat 349

Enkephalin

spinal cord, neurotransmitters, agonists/antagonists, mouse 32

Entorhinal cortex

innervation, nucleus reuniens thalami, neurons, rat 641

stellate cells, potassium currents, rat 1271

Enucleation

corpus callosum, visual projections, hamster 1255

Epilepsy

chronic epileptic foci, neocortex, tetanus toxin, rat 47

epileptiform potentials, hippocampus, guinea-pig 570

Excitatory amino acids

homocysteate, glia, cerebellum, rat 1370

metabotropic receptors, thalamus, neurons, *trans*-1-amino-cyclopentyl-1,3-dicarboxylic acid, effects, rat 1104

microtubules, neurons, rat 551

synaptic potentials, hippocampus, postnatal development, rat 301

Facial motor nucleus

neurons, regeneration, calcitonin gene-related peptide, rat 338

Forebrain

immediate early genes, expression, learning, chick 162

Forelimb

locomotion, X-rays, cat 18

Fos

brain, convulsants, mouse 764

induction, astrocytes, calcitonin gene-related peptides, rat 708

induction, neurons, sympathetic, nerve growth factor, rat 698

induction, spinal cord, sciatic nerve, section, rat 887

G proteins

auditory system, guinea-pig 1338

GABA

neurons, dorsal motor vagal nucleus, nucleus ambiguus, nucleus tractus solitarius, cat 501

receptors, nociception, mouse 833

receptors, oligodendrocytes, developmental regulation, mouse 310

receptors, presynaptic inhibition, primary afferents, crayfish 1208

receptors, presynaptic inhibition, spinal cord, motor neurons, lamprey 107

receptors, thalamus, immunohistochemistry, rat 118

superior colliculus, cerebral cortex, caudate-putamen, lesions, rat 971

synaptic potentials, hippocampus, excitatory amino acids, rat 301

Genes

choline acetyltransferase, expression, cell transfection, rat 1309

ciliary neurotrophic factor, expression, mapping, wobbler, mouse 1182

gene expression, immediate early genes, forebrain, learning, chick 162

gene transfer, human neurofilament-light, neurons, transplantation, hippocampus, rat 758

Giant neurons

ultrastructure, desheathing, calcium currents, *Aplysia* 10

Glia

antigenic determinants, monoclonal antibodies, Japanese quail 126

astrocytes, potassium channels, endothelins, rat 349

cerebral cortex, *in vitro* culture, bioelectric activity, rat 140

differentiation, growth-associated proteins, rat 876

glia-derived nexin, axons, growth, neuroepithelium, man 663

microglia, retina, degeneration, rat 1189

potassium channels, neural adhesion molecules, mouse 230

potassium channels, optic nerve, frog 813

Glutamate

arachidonic acid, metabolites, release, mouse 928

hippocampus, depolarization, rat 1281

microtubules, neurons, rat 551

optic tectum, retinotectal pathway, pigeons 366

receptors, long-term potentiation, perforant path, rat 1300

receptors, potassium channels, activation, cerebellum, mouse 778

Glycoproteins

cerebrum, long-term memory, chicken 243

extracellular matrix, neurons, adhesion, divalent cations, mouse 356

Granule cells

cerebellum, calcium currents, rat 771

cerebellum, potassium channels, activation, mouse 778

Growth-associated proteins

macroglia, differentiation, rat 876

Guanine nucleotide binding proteins

auditory system, guinea-pig 1338

Head

movement, non-saccadic, superior colliculus, rat 790

Hippocampus

calbindin, calcium, homeostasis, age, rat 839

depolarization, excitatory amino acids, rat 1281

epileptiform potentials, guinea-pig 570

gene transfer, human neurofilament-light, neurons, transplantation,

- rat 758
- locus coeruleus, fetal, grafting, microdialysis, rat 905
- N*-methyl-D-aspartate, receptors, excitatory postsynaptic potentials, long-term potentiation, guinea-pig 850
- N*-methyl-D-aspartate, receptors, L-homocysteate, rat 962
- neurons, cholinergic, neurite growth inhibitors, rat 825
- neurons, degeneration, quinolinic acid, rat 40
- neurons, toxicity, α -amino-3-hydroxy-5-methyl-4-isoxazolepropionate, rat 715
- neurons, toxicity, α -amino-3-hydroxy-5-methyl-4-isoxazolepropionate, rat 729
- pyramidal cells, local circuits, rat 587
- pyramidal neurons, potassium conductance, cholinergic/noradrenergic agonists, guinea-pig 473
- Schaffer collaterals, excitatory postsynaptic potentials, *N*-methyl-D-aspartate, receptors, rat 602
- spontaneous miniature postsynaptic currents, potassium currents, mast cell degranulating peptide, rat 523
- Homocysteate**
 - glia, cerebellum, rat 1370
- L-Homocysteate**
 - N*-methyl-D-aspartate, receptors, hippocampus, rat 962
- Hypothalamus**
 - neuropeptides, rat 175
 - suprachiasmatic nucleus, reinnervation, neurons, serotonergic, rat 1330
- Inverted cells**
 - cerebral cortex, retrograde labelling, rabbit 415
- Ionomycin**
 - arachidonic acid, metabolites, release, mouse 928
- Iron**
 - uptake, sciatic nerve, regeneration, rat 919
- Knee**
 - inflammation, spinal cord, neuronal activity, *N*-methyl-D-aspartate, antagonists, cat 981
- Lateral suprasylvian area**
 - binocular interactions, strabismus, corpus callosum, section, cat 1016
- Learning**
 - anoxia, calcium, antagonists, rat 168
 - gene expression, immediate early genes, forebrain, chick 162
- Locomotion**
 - acetylcholinesterase, release, substantia nigra, guinea-pig 292
 - D-1 dopamine receptors, cerebral cortex, amphetamine, rat 1001
 - fictive, interjoint reflexes, crayfish 1219
 - forelimb, X-rays, cat 18
 - spinal cord, neurons, isolation, embryos, *Xenopus* 1025
- Locus coeruleus**
 - catecholamines, sciatic nerve, stimulation, rat 397
 - fetal, grafting, hippocampus, microdialysis, rat 905
- Long-term potentiation**
 - excitatory postsynaptic potentials, *N*-methyl-D-aspartate, receptors, hippocampus, guinea-pig 850
 - perforant path, *N*-methyl-D-aspartate, receptors, rat 1300
- Macrophages**
 - brain, cytotoxicity, neurons, rat 1155
- Mast cell degranulating peptide**
 - Spontaneous miniature postsynaptic currents, potassium currents, pyramidal neurons, rat 523
- Measles virus**
 - neurons, degeneration, *N*-methyl-D-aspartate, receptors, mouse 66
- Medial geniculate nucleus**
 - thalamic reticular nucleus, primate: *Galago* 1089
- Medulla oblongata**
 - neuropeptides, rat 175
 - reticular formation, descending projections, substantia nigra, rat 260
 - spinal cord, descending pathways, synapses, ultrastructure, rat 55
- Memory**
 - Long-term memory, glycoproteins, cerebrum, chicken 243
 - visual, long-term, thalamus, mediodorsal, lesions, cynomolgus monkey 615
- Microtubules**
 - microtubule-associated proteins, brain, cat 1134
 - neurons, excitatory amino acids, rat 551
- Mitral cells**
 - projections, anterograde tracing, rat 493
- Motor neurons**
 - abducens, intracellular recording, *N*-methyl-D-aspartate, rat 621
 - cell death, nerve-muscle interactions, rat 216
 - interjoint reflexes, fictive locomotion, crayfish 1219
 - spinal cord, lesions, calcitonin gene-related peptide, rat 737
 - spinal cord, nerve growth factor, messenger RNA, embryos, rat 953
 - spinal cord, presynaptic inhibition, GABA, receptors, lamprey 107
- Mutations**
 - wobbler, genes, ciliary neurotrophic factor, expression, mouse 1182
- N*-methyl-D-aspartate**
 - antagonists, spinal cord, neuronal activity, knee, inflammation, cat 981
 - excitatory postsynaptic potentials, thalamus, rat 296
 - motor neurons, abducens, intracellular recording, rat 621
 - receptors, epileptiform activity, neocortex, rat 992
 - receptors, excitatory postsynaptic potentials, long-term potentiation, hippocampus, guinea-pig 850
 - receptors, excitatory postsynaptic potentials, Schaffer collaterals, rat 602
 - receptors, hippocampus, L-homocysteate, rat 962
 - receptors, long-term potentiation, perforant path, rat 1300
 - receptors, neurons, degeneration, mouse 66
 - receptors, self-stimulation, prefrontal cortex, rat 531
 - rhythmic discharges, nucleus tractus solitarius, swallowing area, rat 1353
- Neocortex**
 - epileptiform activity, calcium channels, antagonists, rat 992
 - neurons, synchronization, tetanus toxin, rat 47
- Nerve growth factor**
 - Fos, induction, neurons, sympathetic, rat 698
 - messenger RNA, spinal cord, motor neurons, embryos, rat 953
 - neurons, reticular thalamic nucleus, age, rat 1008
- Neural adhesion molecules**
 - potassium channels, glia, mouse 230
- Neural grafting**
 - striatum, ibotenic acid lesions, mouse 86
 - striatum, reinnervation, mouse 72
- Neuroblastoma**
 - cell lines, calcium currents, man 514
 - cell lines, neural adhesion molecules, cross-linking, mouse 634
 - receptors, muscarinic receptors, M-current 820
- Neuroepithelium**
 - axons, growth, serine proteases, man 663
- Neurogenetic gradients**
 - retina, fowl 559
- Neuromasts**
 - distribution, neuropeptides, *Astyanax jordani* 407
- Neuromodulin**
 - macroglya, differentiation, rat 876
- Neurons**
 - adhesion, glycoproteins, extracellular matrix, calcium, zinc, mouse 356
 - arachidonic acid, metabolites, release, mouse 928
 - auditory cortex, responses, complex sounds, bat 1165
 - C-fibres, regeneration, capsaicin, rat 274
 - cell death, retina, microglia, rat 1189
 - cerebral cortex, *in vitro* culture, bioelectric activity, rat 140
 - cholinergic, hippocampus, regeneration, neurite growth inhibitors, rat 825
 - cytotoxicity, macrophages, brain, rat 1155
 - degeneration, C57BL/Ola, mouse 102
 - degeneration, hippocampus, striatum, quinolinic acid, rat 40
 - degeneration, measles virus, *N*-methyl-D-aspartate, receptors, mouse 66
 - dopaminergic, cerebral cortex, locomotion, rat 1001

Subject index

- lifespan, olfactory receptors, mouse 209
- microtubules, excitatory amino acids, rat 551
- motor, regeneration, calcitonin gene-related peptide, rat 338
- neocortex, synchronization, tetanus toxin, rat 47
- neurogenesis, retina, fowl 559
- parietal cortex, visual stimulation, macaque 452
- primary afferents, presynaptic inhibition, GABA, receptors, crayfish 1208
- Purkinje cells, *in vitro* development, embryos, rat 855
- regeneration, proximal nerve stumps, mouse 1366
- reticular thalamic nucleus, nerve growth factor, age, rat 1008
- sensory neurons, calcium, homeostasis, ATP receptors, rat 285
- sensory neurons, peripheral nerves, regeneration, plasticity, dorsal horn, rat 1112
- serotonergic, reinnervation, suprachiasmatic nucleus, rat 1330
- toxicity, α -amino-3-hydroxy-5-methyl-4-isoxazolepropionate, brain, rat 715
- toxicity, α -amino-3-hydroxy-5-methyl-4-isoxazolepropionate, brain, rat 729
- transplantation, hippocampus, gene transfer, human neurofilament-light, rat 758
- Neuropeptides**
 - chromogranins, messenger RNA, brain, rat 895
 - cutaneous sense organs, *Asiyanax jordani* 407
 - morphine-modulating peptides, enkephalin, brain, rat 175
 - N*-acetylasparylglutamate, optic tectum, retina, synaptic release, fowl 441
 - neurons, circumvallate papilla, retrograde tracing, rat 331
- Neurotoxins**
 - mast cell degranulating peptide, spontaneous miniature postsynaptic currents, potassium currents, pyramidal neurons, rat 523
- Neurotransmitters**
 - agonists/antagonists, enkephalin, spinal cord, mouse 32
- Neurotrophic factors**
 - brain-derived neurotrophic factor, messenger RNA, rat 688
 - ciliary neurotrophic factor, genes, mouse 1182
- Nitric oxide**
 - climbing fibres, cerebellum, rat 379
- Nociception**
 - ascending pathways, spinal cord, rat 249
 - GABA, receptors, mouse 833
 - N*-methyl-D-aspartate, antagonists, cat 981
 - nociceptors, skin, capsaicin, rat 274
- Noradrenalin**
 - thalamus, oscillation, adrenoreceptors, rat 222
- Nucleus ambiguus**
 - neurons, GABA, cat 501
- Nucleus reuniens thalami**
 - neurons, entorhinal cortex, innervation, rat 641
- Nucleus ruber**
 - cerebral cortex, projections, guinea-pig 866
- Nucleus tractus solitarius**
 - neurons, GABA, cat 501
 - swallowing area, rhythmic discharges, *N*-methyl-D-aspartate, rat 1353
- Olfactory bulb**
 - mitral cells, olfactory coding, olfactory projections, anterograde tracing, rat 493
 - olfactory receptors, neurons, lifespan, mouse 209
- Oligodendrocytes**
 - differentiation, growth-associated proteins, rat 876
 - GABA, receptors, developmental regulation, mouse 310
- Opioid receptors**
 - dorsal root C7, rat 1343
- Optic nerve**
 - astrocytes, potassium channels, frog 813
 - crushing, retina, reinnervation, ganglion cells, cat 1245
- Optic tectum**
 - N*-acetylasparylglutamate, synaptic release, fowl 441
 - retinotectal pathway, glutamate, pigeon 366
- Orientation**
 - tuning, visual cortex, cat 1232
- Pallidal complex**
 - metabolism, subthalamic nuclei, rat 947
- Parietal cortex**
 - visual area, neurons, visual stimulation, macaque 452
- Parvalbumin**
 - distribution, basal nuclei, squirrel monkey 1316
- Passive avoidance training**
 - glycoproteins, cerebrum, chicken 243
- Perforant path**
 - long-term potentiation, *N*-methyl-D-aspartate, receptors, rat 1300
- Pontine grey**
 - neurons, tuning, echolocation, horseshoe bat 648
- Postsynaptic currents**
 - spontaneous miniature postsynaptic currents, pyramidal neurons, mast cell degranulating peptide, rat 523
- Postsynaptic potentials**
 - excitatory, long-term potentiation, *N*-methyl-D-aspartate, receptors, hippocampus, guinea-pig 850
 - excitatory, Schaffer collaterals, *N*-methyl-D-aspartate, receptors, rat 602
 - excitatory, thalamus, *N*-methyl-D-aspartate, rat 296
 - pyramidal cells, hippocampus, *N*-methyl-D-aspartate, receptors, rat 587
- Potassium**
 - potassium channels, activation, glutamate, receptors, cerebellum, mouse 778
 - potassium channels, astrocytes, endothelins, rat 349
 - potassium channels, astrocytes, potassium channels, frog 813
 - potassium channels, glia, neural adhesion molecules, mouse 230
 - potassium conductance, pyramidal neurons, hippocampus, cholinergic/noradrenergic agonists, guinea-pig 473
 - potassium currents, inactivation, chromaffin cells, cattle 462
 - potassium currents, M-current, muscarinic receptors, neuroblastoma, transfected cells 820
 - potassium currents, pyramidal neurons, mast cell degranulating peptide, rat 523
 - potassium currents, stellate cells, entorhinal cortex, rat 1271
- Prefrontal cortex**
 - self-stimulation, *N*-methyl-D-aspartate, receptors, rat 531
- Projection neurons**
 - cerebral cortex, retrograde labelling, rabbit 415
- Prothrombin**
 - axons, growth, neuroepithelium, man 663
- Proto-oncogenes**
 - expression, forebrain, learning, chick 162
- Purkinje cells**
 - climbing fibre responses, calcium, rat 343
 - in vitro* development, embryos, rat 855
- Pyramidal cells**
 - hippocampus, local circuits, rat 587
 - striate cortex, vertical connections, cat 1
- Pyramidal neurons**
 - hippocampus, potassium conductance, guinea-pig 473
- Reinnervation**
 - striatum, neural grafting, mouse 72
- Reticular thalamic nucleus**
 - neurons, nerve growth factor, age, rat 1008
- Retina**
 - bipolar cells, morphological classification, rhesus monkey 1069
 - degeneration, microglia, rat 1189
 - ganglion cells, degeneration, reinnervation, optic nerve, crushing, cat 1245
 - N*-acetylasparylglutamate, synaptic release, fowl 441
 - neurogenesis, fowl 559
- Retinotectal pathway**
 - glutamate, pigeon 366
- RNA**
 - synthesis, inhibitors, sural nerves, ultrastructure, rat 1123

mRNA

- brain-derived neurotrophic factor, dorsal root ganglia, spinal cord, motor neurons, embryos, rat 953
- brain-derived neurotrophic factor, ontogeny, rat 688
- calcitonin gene-related peptide, motor neurons, spinal cord, lesions, rat 737
- Fos, calcitonin gene-related peptides, rat 708

Saphenous nerve

- connections, sciatic nerve, section, rat 383

Schwann cells

- antigenic determinants, monoclonal antibodies, Japanese quail 126

Sciatic nerve

- regeneration, transferrin receptors, iron uptake, rat 919
- section, saphenous nerve, connections, dorsal horn 383
- stimulation, catecholamines, locus coeruleus, rat 397

Secretogranins

- messenger RNA, brain, rat 895

Self-stimulation

- prefrontal cortex, *N*-methyl-D-aspartate, receptors, rat 531

Serine proteases

- axons, growth, neuroepithelium, man 663

Shape

- somatosensory discrimination, cerebrum, mapping, positron emission tomography, man 481

Skin

- nociceptors, capsaicin, rat 274

Slice cultures

- spinal cord, dorsal root, cytology, rat 1037
- spinal cord, dorsal root, reflex arc, rat 1054

Somatosensory discrimination

- shape, cerebrum, mapping, positron emission tomography, man 481

Somatostatin

- thalamic reticular nucleus, *Galago* 237

Sound

- complex sounds, auditory cortex, responses, bat 1165

Spectrins

- brain spectrins, dorsal root ganglia, development, fowl 431

Spinal cord

- ascending pathways, visceroreception/nociception, rat 249
- dorsal root, slice cultures, reflex arc, cytology, rat 1037
- dorsal root, slice cultures, reflex arc, rat 1054
- Fos, induction, sciatic nerve, section, rat 887
- lesions, calcitonin gene-related peptide, rat 737
- medulla oblongata, descending pathways, synapses, ultrastructure, rat 55
- motor neurons, nerve growth factor, messenger RNA, embryos, rat 953
- motor neurons, presynaptic inhibition, GABA, receptors, lamprey 107
- neuronal activity, *N*-methyl-D-aspartate, antagonists, knee, inflammation, cat 981
- neurons, enkephalin, neurotransmitters, agonists/antagonists, mouse 32
- neurons, isolation, locomotion, embryos, *Xenopus* 1025
- opioid receptors, dorsal root C7, rat 1343

Strabismus

- lateral suprasylvian area, binocular interactions, corpus callosum, section, cat 1016

Striate cortex

- afferent connections, cat 186
- vertical connections, cat 1

Striatum

- ascorbate, release, dopamine, receptors, rat 940
- astrocytes, calcium, adrenoreceptors, adenosine, mouse 539
- neural grafting, ibotenic acid lesions, mouse 86
- neurons, degeneration, quinolinic acid, rat 40
- reinnervation, neural grafting, mouse 72

Substantia nigra

- acetylcholinesterase, release, light-emitting reaction, locomotion, guinea-pig 292
- descending projections, medulla oblongata, reticular formation, rat 260
- metabolism, subthalamic nuclei, rat 947

Subthalamic nuclei

- pallidal complex, substantia nigra, metabolism, rat 947

Superior colliculus

- GABA, caudate-putamen, cerebral cortex, lesions, rat 971
- head, movement, non-saccadic, rat 790

Suprachiasmatic nucleus

- reinnervation, neurons, serotonergic, transplantation, rat 1330

Sural nerves

- ultrastructure, RNA, synthesis, inhibitors, rat 1123

Synapses

- cyclic AMP, binding sites, brain, rat 669

Synaptic potentials

- GABA, hippocampus, excitatory amino acids, rat 301

Tactile exploration

- cerebrum, mapping, positron emission tomography, man 481

Taste buds

- distribution, neuropeptides, *Astyanax jordani* 407

Tau proteins

- brain, cat 1134

Temporal cortex

- connections, horseradish peroxidase, rat 317

Tetanus toxin

- chronic epileptic foci, rat 47

Tetradotoxin

- bioelectric activity, cerebral cortex, rat 154

Thalamic reticular nucleus

- auditory cortex, thalamus, projections, bushbabies 1089

Thalamus

- excitatory postsynaptic potentials, *N*-methyl-D-aspartate, rat 296
- GABA, receptors, immunohistochemistry, rat 118
- mediodorsal, lesions, memory, visual, long-term, cynomolgus monkey 615
- neurons, excitatory amino acids, metabotropic receptors, *trans*-1-amino-cyclopentyl-L-3-dicarboxylic acid, effects, rat 1104
- oscillation, adrenoreceptors, noradrenalin, rat 222

Thrombin

- axons, growth, neuroepithelium, man 663

Tongue

- circumvallate papilla, neurons, retrograde tracing, rat 331

Transferrin

- receptors, sciatic nerve, regeneration, rat 919

Visceroreception

- ascending pathways, spinal cord, rat 249

Visual cortex

- neurons, visual stimulation, macaque 452
- orientation, tuning, cat 1232
- tau proteins, distribution, cat 1134